

WOODS HOLE OCEANOGRAPHIC INSTITUTION

Woods Hole, Massachusetts

In citing this MANUSCRIPT in a
bibliography, the reference should
be followed by the phrase:
UNPUBLISHED MANUSCRIPT.

AD14994

Reference No. 53-48

The Growth of Sea Salt
Particles by Condensation
Of Atmospheric Water Vapor

by

C. H. Keith

and

A. B. Arons

Technical Report No. 5
submitted to Geophysics Branch
Office of Naval Research
under Contract No. Nonr-798 (00) (NR-085-001)

June 1953

APPROVED FOR DISTRIBUTION

10/2/53

Director

Abstract

Measurements of the rate of growth of sea salt particles have been made when the particle is shifted from an environment of dry air to one of relative humidity between 80 and 100 percent. For particles ranging from 10^{-9} to 2×10^{-8} grams mass, agreement is found with growth times predicted by an equation which principally differs from previous derivations in that empirical vapor pressure data are utilized. The growth time is observed to be independent of ventilation at air speeds less than 30-40 centimeters per second.

The growth equation was reintegrated under variable humidity and temperature conditions corresponding to rates of rise observed in the atmosphere. The curves thus obtained approximately trace the growth of sea salt particles rising from the sea surface to cloud base.

I Introduction:

Accurate information about the growth of microscopic sea salt particles by condensation of water vapor is necessary for the evaluation of the role of these particles in the formation of clouds, rain, and fog. Condensational growth has been the subject of theoretical investigations by Howell (1949), Kraus and Smith (1949), Squires (1952), Best (1953), and others. In these investigations, the use of Raoult's law, and of various other approximations, made the accuracy of the resulting growth calculations doubtful.

Since Woodcock (1949, 1952) has demonstrated the presence of large sea salt nuclei (10^{-8} to 10^{-12} grams) in the atmosphere, and since his subsequent investigations indicate that these nuclei may possibly play a dominant role in the mechanism of rain production in warm clouds, it was felt that a careful experimental and theoretical investigation of the growth of droplets formed on such nuclei was desirable. The application of the derived growth equation under variable temperature and humidity conditions was also considered, so that a droplet size spectrum in sub-cloud regions may be obtained from the resultant growth curves and from Woodcock's (1949, 1952) salt particle distributions.

III The growth equation:

In previous investigations, Howell (1949) and others were concerned with nuclei having masses of 10^{-13} to 10^{-20} grams which were growing in an atmosphere super-

saturated with water vapor. With such small particles, the effect of surface tension on the droplet vapor pressure was of the same or greater magnitude than the lowering caused by dissolved salts. For droplets of the size with which we are here concerned, surface tension effects are negligible, and the humidity range of interest is that below 100%. During much of its growth, the droplet consists of a concentrated solution of sea salt for which the vapor pressure deviates appreciably from that given by Raoult's law. For this reason, the recently reported vapor pressure measurements of Arons and Kientzler (1953) have been empirically incorporated in the theoretical part of our investigation.

If a sea salt particle is introduced into an atmosphere of sufficiently high relative humidity, the particle will grow to a droplet by condensation of water vapor. Growth will continue until an equilibrium size is reached, when the droplet vapor pressure is equal to that of water in the surrounding atmosphere. The growth rate depends primarily upon the vapor pressure gradient between the droplet surface and ambient air. This gradient determines the rate of vapor diffusion to the saline surface of the droplet, and consequently the rate of condensation. The heat liberated by condensation is initially stored in the droplet, hence elevating its temperature. This has the dual effect of reducing the vapor gradient and allowing heat conduction away from the

droplet. In the following derivation it is assumed that a steady state condition in which the vapor and thermal gradients are interdependent is rapidly obtained. It is also assumed that the classical laws of diffusion and heat conduction apply to these droplets. Howell (1949) has discussed the limits of applicability of these laws and concludes that kinetic theory correction need not be made for droplets of radius greater than 6-8 microns.

It is further assumed that the effect of other droplets upon the gradients around a given droplet is negligible, and that mass divergence is also negligible in the initial transport equations. These have also been considered by Langmuir (1944) and Howell (1949), and found to be reasonable assumptions.¹

The well known rate equations are:

$$\frac{dq}{dt} = \text{time rate of mass transport of water vapor to the droplet} = 4\pi D (R')^2 \left[\frac{d\rho}{dR'} \right] \quad (1)$$

$$\frac{dQ_1}{dt} = \text{time rate of heat transport away from the droplet} = 4\pi k (R')^2 \left[\frac{dT}{dR'} \right] \quad (2)$$

$$\frac{dQ_2}{dt} = \text{time rate of heat storage in the droplet} = mc_p \frac{dr}{dt} \frac{dT}{dT} \quad (3)$$

¹ See Appendix I for a list of the symbols used throughout this report.

Integration of (1) and (2) over space leads to the usual expressions for the thermal and vapor density gradients between r , the droplet radius, and a point infinitely removed from r . It is also assumed that all the vapor which diffuses to the droplet is condensed thereon, i.e., that the accommodation coefficient is unity. Substitution of the thermal and vapor gradients in the above equations leads to the heat and vapor balance equation,

$$LD(\rho_1 - \rho) = \left(k + \frac{1}{3} \rho_s c_p r \frac{dr}{dt} \right) (T - T_1) \quad (4)$$

The vapor transport equation (1) may be transformed into the well known form which gives the time rate of change to droplet radius in terms of the vapor density gradient,

$$r \frac{dr}{dt} = \frac{D}{\rho_s} (\rho_1 - \rho) \quad (5)$$

Combination of this with (4), and conversion of vapor density to vapor pressure by means of the ideal gas law yields

$$r \frac{dr}{dt} = \frac{DM}{\rho_s R} \left(\frac{P_1}{T_1} - \frac{P}{T} \right) = \left(\frac{k}{\rho_s L} + \frac{c_p}{3L} r \frac{dr}{dt} \right) (T - T_1) \quad (6)$$

The Clapeyron equation, in its integrated form, can be used to describe the variation of droplet vapor pressure, p , with droplet temperature, T :

$$\ln \frac{P}{P_2} = \frac{LM}{R} \left(\frac{1}{T_1} - \frac{1}{T} \right) \quad (7)$$

Since the pressure and temperature differences are small, equation (7) may be approximated by:

$$P = P_2 \left[1 + \frac{LM}{RT_1^2} (T - T_1) \right] \quad (8)$$

By rearranging the first and last terms of (6), an expression for T in terms of T_1 and $r \frac{dr}{dt}$ is obtained.

$$T = T_1 + \frac{P_2 L}{k \alpha} r \frac{dr}{dt} \quad (9)$$

where

$$\alpha \equiv 1 + \frac{C_p P_2}{3k} r \frac{dr}{dt}$$

Substitution of (8) and (9) for P and T in the second term of (6) yields:

$$r \frac{dr}{dt} = \frac{DM}{P_2 R} \left\{ \frac{P_1}{T_1} - P_2 \left(1 + \frac{P_2 L^2 M}{k \alpha R T_1^2} r \frac{dr}{dt} \right) \left(T_1 + \frac{P_2 L}{k \alpha} r \frac{dr}{dt} \right)^{-1} \right\} \quad (10)$$

which, upon rearrangement and solution of the resulting quadratic equation gives:

$$r \frac{dr}{dt} = B(p) \left\{ 1 \pm \left[1 + \frac{C(p)}{B^2(p)} \right]^{\frac{1}{2}} \right\} \quad (11)$$

where $B(p) \equiv \frac{DM}{2P_2 R T_1} \left(P_1 - \frac{MLP_2}{RT_1 Y} P_2 - \frac{RT_1^2 k}{DMLY} \right)$

$$C(p) \equiv \frac{DM}{RLP_2^2 Y} (P_1 - P_2)$$

$$\gamma \equiv 1 + \frac{C_p T_1}{3L} \quad \beta \equiv 1 + \frac{C_p R T_1^2}{3ML^2}$$

Examination of (11) shows that $C(p)$ is positive during droplet growth because of the positive vapor pressure gradient necessary for growth. Evaluation of the expression $\frac{ML\phi}{RT_1\gamma}$ shows that the second term of $B(p)$ is approximately 16 times the leading term, hence $B(p)$ is inherently negative. Since $r \frac{dr}{dt}$ must be positive for growth to occur, the negative branch of (11) is the one having physical significance in the present problem.

Since p_1 is defined as the ambient vapor pressure, it is equal to the product of the relative humidity and the saturation vapor pressure, p_0 . The vapor pressure of the droplet at the ambient temperature, p_2 , can be considered as the difference between p_0 and the vapor pressure lowering, Δp . The vapor pressure lowering is, of course, a function of temperature and the concentration of the droplet.

Droplet concentration is thus indirectly introduced into (11), and since this is conveniently expressed in terms of the weight of salt per weight of solution, it would generalize (11) to introduce in place of r a concentration variable. This would remove any explicit dependence upon particle weight from the growth equation. Such a variable is the "scaled" radius,

$$\sigma = rm_s^{-1/3} \quad (12)$$

and this requires the further substitution of a "scaled" time,

$$\tau = tm_s^{-1/3} \quad (13)$$

in place of t so that

$$r \frac{dr}{dt} = \sigma \frac{d\sigma}{d\tau} \quad (14)$$

With these changes equation (11) assumes the form

$$\sigma \frac{d\sigma}{d\tau} = B(\sigma) \left\{ 1 - \left[1 + \frac{C(\sigma)}{B(\sigma)} \right]^{\frac{1}{2}} \right\} \approx -\frac{C(\sigma)}{2B(\sigma)} + \frac{C^2(\sigma)}{8B^3(\sigma)} - \frac{C^3(\sigma)}{16B^5(\sigma)} + \dots \quad (15)$$

where

$$B(\sigma) \equiv \frac{DM}{2\rho_s RT_1} \left\{ \left(H - \frac{ML\beta}{RT_1\gamma} \right) P_0 + \frac{ML\beta}{RT_1\gamma} \Delta P(\sigma) - \frac{RT_1^2 k}{DML\gamma} \right\}$$

$$C(\sigma) \equiv \frac{DMK}{RL\rho_s^2\gamma} \left\{ (H-1) P_0 + \Delta P(\sigma) \right\}$$

Evaluation of the terms on the right hand side of equation (15) shows that the second term is less than .05 percent of the leading term. Since Arons and Kientzler (1953) estimate a 2% error in the vapor pressure data, equation (15) can be sufficiently well approximated as

$$\sigma \frac{d\sigma}{d\tau} = \left\{ (H-1) P_0 + \Delta P(\sigma) \right\} \left\{ \frac{\rho_s RT_1}{DM} + \frac{ML^2 \rho_s \beta}{RT_1^2 k} \left[P_0 - \Delta P(\sigma) \right] - \frac{L \rho_s \gamma}{k T_1} H P_0 \right\}^{-1} \quad (16)$$

An important assumption contained in the foregoing development is that the water condensed upon the droplet quickly reaches a salinity equivalent to that of a completely mixed droplet. At any early stage in the experimental work, disagreement between calculated and experimental

growth times led to the investigation of the possibility that outward salt diffusion might be the controlling factor in growth. A theoretical treatment of this situation revealed, however, that times of the order of several milliseconds were sufficient for molecular diffusion to produce essentially complete homogeneity within the droplet. Internal salt diffusion was therefore ruled out as a controlling factor in droplet growth, since actual growth times were known to be of the order of tens of seconds.

Before proceeding further with the development of the growth equation, it is necessary to formulate an empirical vapor pressure equation for $\Delta p(\sigma)$. σ is given in terms of the density and concentration of the solution by the following relation:

$$\sigma = \left\{ \frac{3}{4\pi\rho_s} \left(1 + \frac{m_w}{m_s} \right) \right\}^{\frac{1}{3}} \quad (17)$$

In (17) the mass of water, m_w , equals 1000-1.805 Cl, and the mass of salt, m_s , equals 1.805 Cl, the chlorinity units being parts per thousand. Arons and Kientzler's (1953) smoothed vapor pressure data are plotted against σ in Fig. 1, and the following empirical representation is obtained:

$$\Delta p(\sigma) = .146 p_0 \sigma^{-3.35} \quad (18)$$

Unfortunately, the non-integral power of σ in $\Delta p(\sigma)$ prohibits analytical integration of (16) at any value

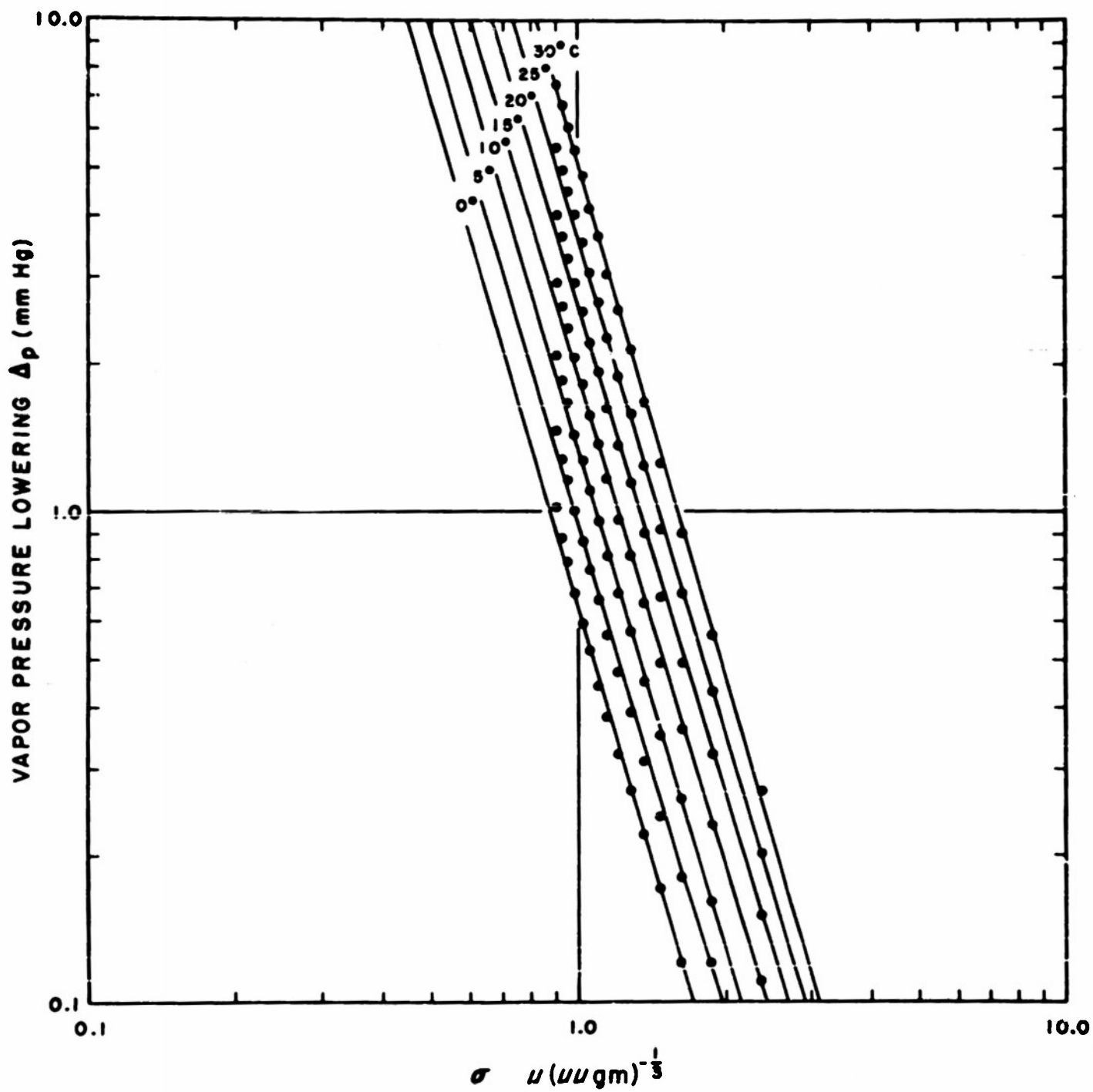


Fig. 1. Kientzler and Arons' vapor pressure lowerings for sea salt solutions presented as a function of sigma ($\sigma = \text{rm}_s^{-1/3}$). The lines are calculated by the equation $\Delta p(\sigma) = .146 p_0 \sigma^{-3.35}$

of the humidity, H, besides 1.0. At this value the integration yields the expression:

$$1.28 \left(\frac{p_s RT_1}{DM p_s} + \frac{ML^2 A \beta}{RT_1^2 k} - \frac{LA \gamma}{k T_1} \right) \sigma^{5.35} - \frac{ML^2 A \beta}{2 RT_1^2 k} \sigma^2 = \tau + C \quad (19)$$

Since it is necessary to integrate the growth equation numerically at other humidities, further simplification of (16) is desirable in order to reduce the labor involved. The difference between $H p_0$ and $p_0 - \Delta p(\sigma)$ is normally small, hence it is convenient to introduce:

$$\ln \frac{H p_0}{p_0 - \Delta p(\sigma)} \cong [(H-1) p_0 + \Delta p(\sigma)] [\bar{p}]^{-1}$$

where \bar{p} = the mean of the ambient and droplet vapor pressures. Also, by ignoring the heat storage within the droplet and calling the ratios of $H p_0 / \bar{p}$ and $p_0 - \Delta p(\sigma) / \bar{p}$ unity, equation (16) reduces to

$$\sigma \frac{d\sigma}{d\tau} = -A \ln \frac{1 - .146 \sigma^{-2.35}}{H} \quad (20)$$

where

$$A \equiv \left(\frac{p_s RT_1}{DM \bar{p}} + \frac{p_s ML^2}{RT_1^2 k} - \frac{p_s L}{k T_1} \right)^{-1}$$

Substitution of values of the indicated constants leads to values of A which are relatively insensitive to changes in \bar{p} . For example, at 25°C, \bar{p} can vary from 19 to 24 millimeters of mercury which amounts to a variation in A of $\pm 0.7\%$ about the mean. However, A is quite temperature sensitive, as is shown in the following Table.

Table I

Values of the factor A in equation (20)
at various temperatures

T°C	A ($\text{cm}^2 \text{ sec}^{-1}$)
0	55
10	83
20	114
30	143

Equation (20) is essentially the same as Howell's (1949), except that surface tension effects have been neglected and an empirical vapor pressure function introduced. Before comparison of (16), the more exact form, with (20), it is necessary to define the limits of integration.

The upper limit of σ , or its equilibrium value, is defined by both equations (16) and (20). In each equation, the right hand side approaches zero as $.146\sigma^{-3.35}$ approaches 1-H, hence τ approaches infinity asymptotically. Comparison of values obtained by

$$\sigma_{eq} = \left(\frac{.146}{1-H} \right)^{.299} \quad (21)$$

with those calculated by the formula developed by Wright (1936) reveals that his values are from 3 to 14% greater than those computed by (21). The reason for this discrepancy is contained in Wright's (1936) use of a constant "hygroscopic factor" in Raoult's law. McDonald (1953) has discussed the use of such factors which account for the

ionic character of salt solutions, and he demonstrates that considerable error may be introduced either by neglecting them entirely or by not considering their variation with concentration. Comparison of the vapor pressure lowerings of sea salt solutions with those of sodium chloride solutions reveals that the former exhibit greater deviations from an ideal completely dissociated solution, i.e. the Bjerrum g factor is lower over the whole concentration range. This is undoubtedly caused by the complex nature of solutions of sea salt, which contains both monovalent and divalent ions.

Since growth originates with a solid particle, and (18) only applies to solutions, an additional vapor pressure function must be derived for the initial period of growth from particle to saturated solution. Unfortunately, data on the vapor pressures over moist sea salt is unavailable, and a reasonable approximation must be employed. Data reported by Thompson (1932) on the composition of salts deposited by evaporation of sea water shows that the final salt crystalized is bischofite ($\text{MgCl}_2 \cdot 6 \text{H}_2\text{O}$). It is therefore to be expected that the first water condensed upon a dessicated sea salt particle will form a film of solution saturated with magnesium chloride. For the purposes of this development it is assumed that, during crystal growth, the vapor pressure rises linearly from that above a saturated magnesium chloride solution to that above a saturated sea salt solution.

Calculation of the values of σ for the crystal and saturated droplet is also necessary. Arons and Kientzler (1953) found that a chlorinity of 156 parts per thousand corresponds to saturation at 25°C. This information, when combined with density data from Higashi (1931) in equation (17) leads to a value of 0.90 microns (micromicrograms)^{-1/3} for a saturated droplet. Sigma for the crystal is computed from the density and weight of hydrated water by equation (17). The density of sea salt can be computed from the weights and densities of the salts present in the mixture. This is accomplished by calculation of the relative weight and volume of each salt present and by division of the total weight by total volume of salts. Using the data reported by Thompson, a value of 2.06 grams per cubic centimeter is obtained. The value of σ calculated from this density is 0.50 microns (micromicrograms)^{-1/3}. The International Critical Tables give 33% as the value of relative humidity over saturated MgCl_2 solution. Making use of equation (18) and the values of σ estimated above, one obtains the following expression for the vapor pressure during the change from crystal to saturated sea salt solution, i.e. for the range $0.50 < \sigma < .90$:

$$\Delta p(\sigma) = p_0(1.25 - 1.16\sigma) \quad (22)$$

Substitution of (22) into (16), evaluation of the constants, and integration, result in the following equation, which

gives the scaled time, τ_0 , for growth to a saturated sea salt solution at 25°C.

$$\tau_0 = (.0013 + .0043H) \left[-.46 + (H + .25) \ln \frac{H - .93}{H - .79} \right] - .0017 \quad (23)$$

Values of τ_0 computed by (23) are listed in Table II.

Table II

Scaled time for growth of sea salt particles
to droplets of saturated solution as a
function of relative humidity.
 $T_1 = 25^\circ\text{C}$

H	$\tau_0, \text{sec } (\mu\mu \text{ gm})^{-2/3}$
.85	.0077
.90	.0057
.92	.0052
.94	.0048
.96	.0044
.98	.0041
.99	.0040
1.0	.0038

The numerical integration of the growth equations (16) and (20) was performed by the usual trapezoidal area method. By substitution of $\frac{\Delta\sigma}{\Delta\tau}$ for $\frac{d\sigma}{d\tau}$ in (16) and (20) and choice of a suitably small increment $\Delta\sigma$ (.01 - .05 microns (micromicrograms)^{-1/3}), $\Delta\tau$ was obtained from the mean value of $\frac{\Delta\sigma}{\Delta\tau}$ in the interval $\Delta\sigma$. The sum of the preceding increments, $\Delta\tau$, gave the value of τ for a given σ . The results of these integrations are presented in Tables III and IV, and Figs. 2 and 3.

Comparison of equation (19) with equation (20) at $H = 1.0$
(excluding τ_0 for growth of crystal)

σ $\mu(\mu\text{gms})^{1/3}$	$\tau(19)$ $T_1 = 25^\circ\text{C}$ $\text{sec}(\mu\text{gms})^{1/3}$	$\tau(20)$ $T_1 = 25^\circ\text{C}$ $\text{sec}(\mu\text{gms})^{1/3}$	$\tau(20)$ $T_1 = 30^\circ\text{C}$ $\text{sec}(\mu\text{gms})^{1/3}$	$\tau(20)$ $T_1 = 20^\circ\text{C}$ $\text{sec}(\mu\text{gms})^{1/3}$
.9				
1.0	.0036	.0039	.0035	.0045
1.2	.0184	.0196	.0176	.0222
1.4	.0501	.0525	.0471	.0595
1.6	.111	.114	.103	.130
1.8	.215	.222	.199	.252
2.0	.384	.396	.355	.449
2.2	.648	.665	.596	.754

The close agreement between the results obtained with equations (19) and (20) justifies the use of the simplified form, equation (20), in subsequent calculations.

[illegible]

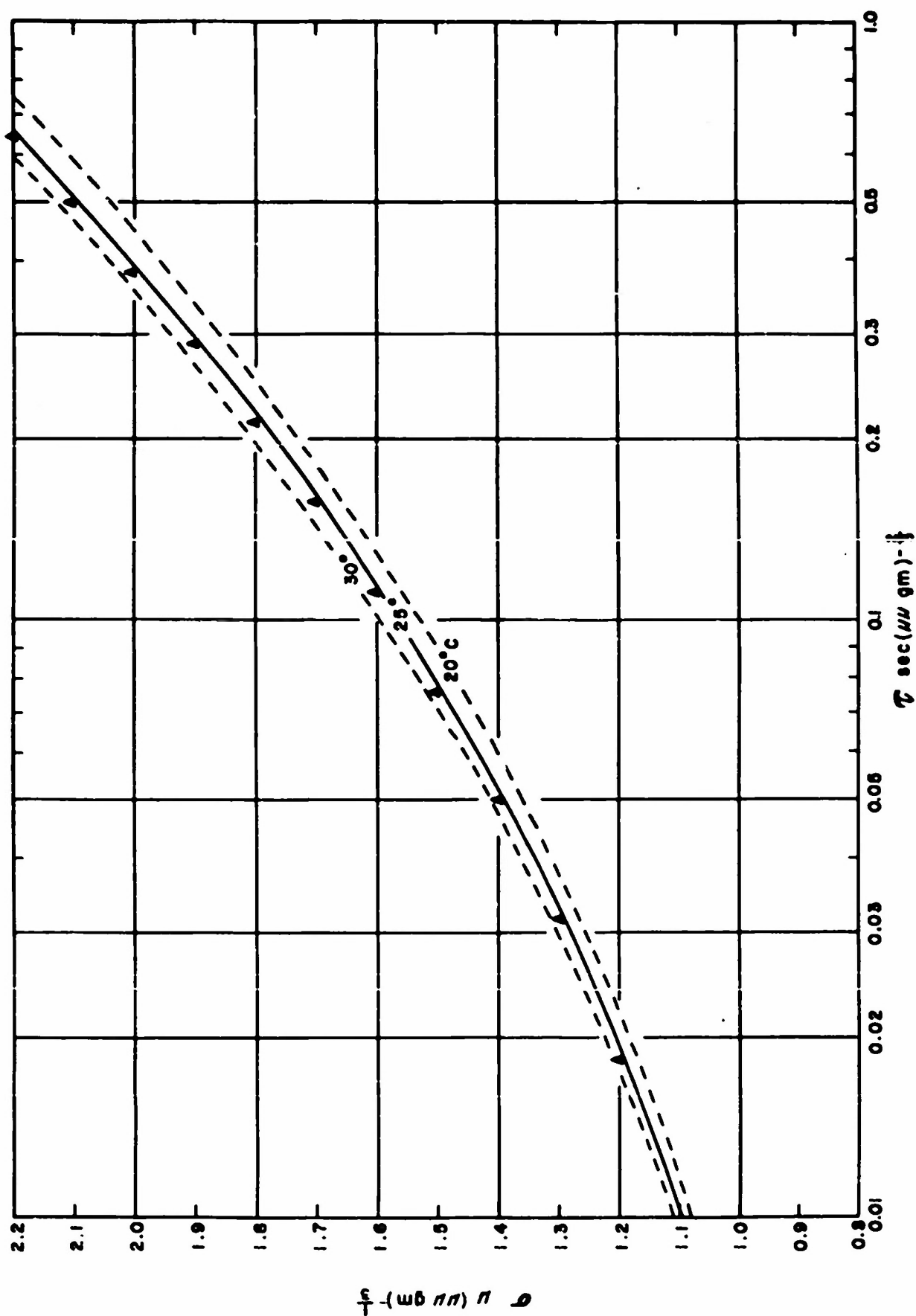


Fig. 2. Comparison of the growth curves obtained from equations (19) and (20) at saturation. T_0 , the scaled time for crystalline growth is not included. The solid line represents values calculated by an approximate growth equation (20), and the triangles those calculated by (19). The dashed lines indicate the variation of equation (20) with temperature.

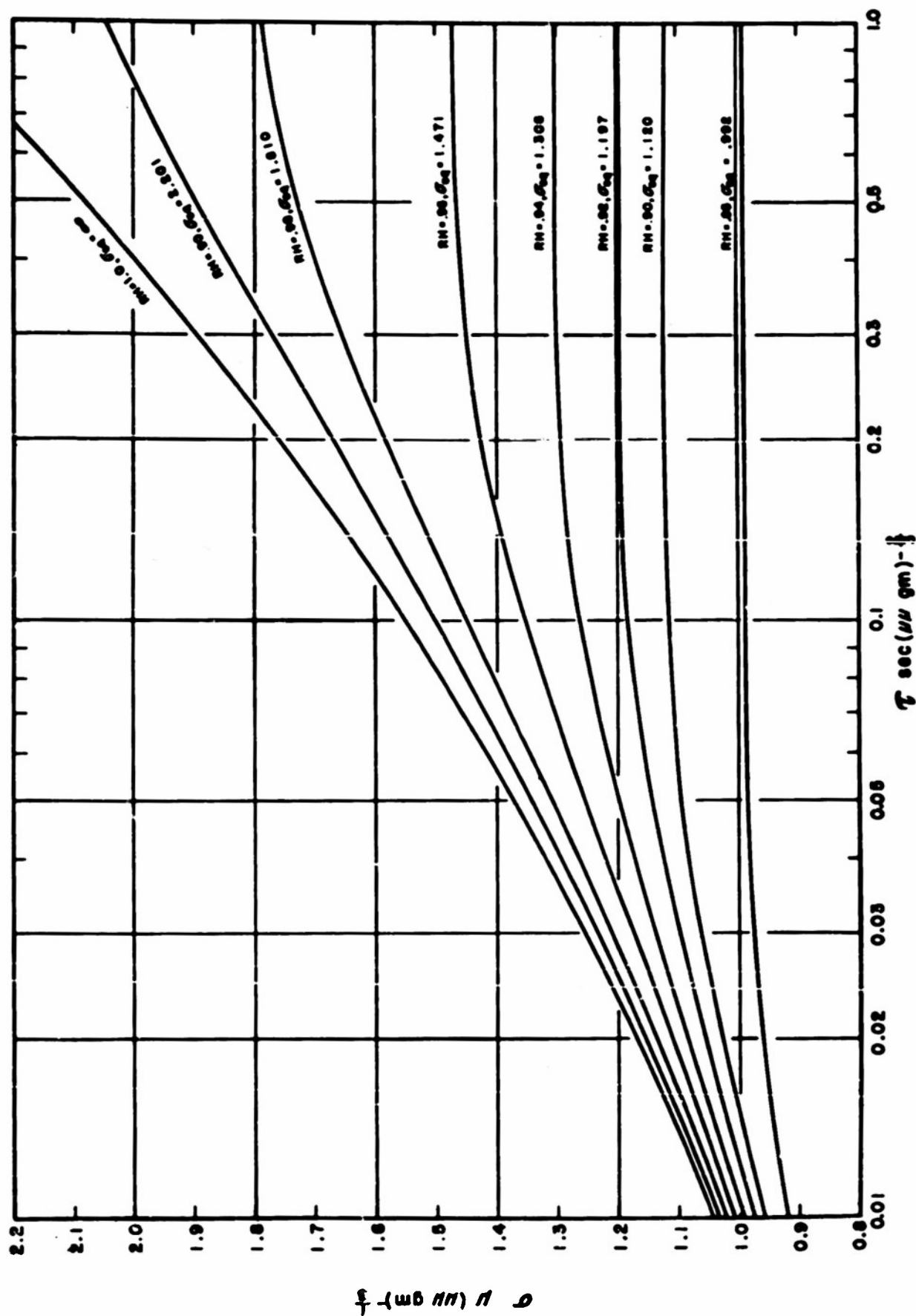
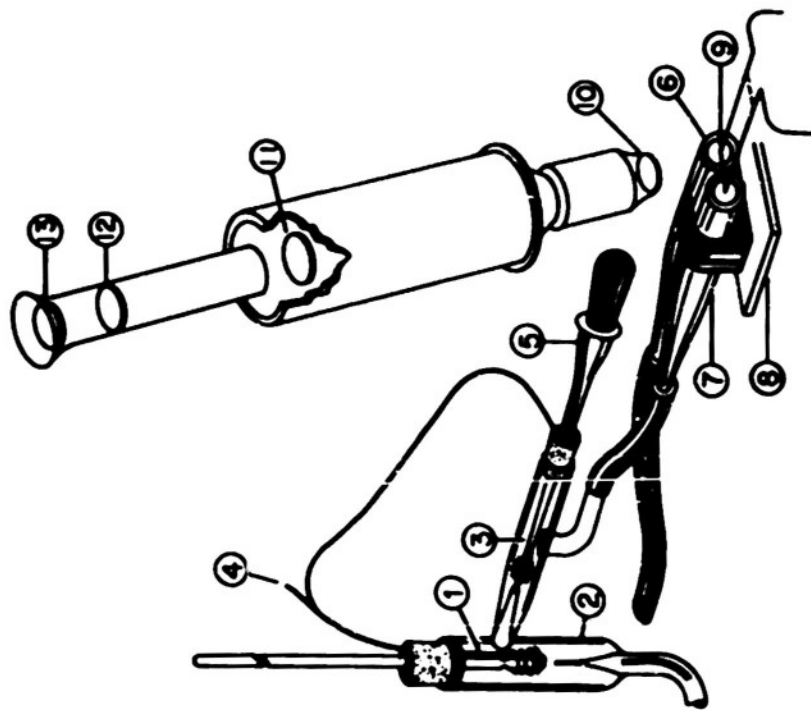
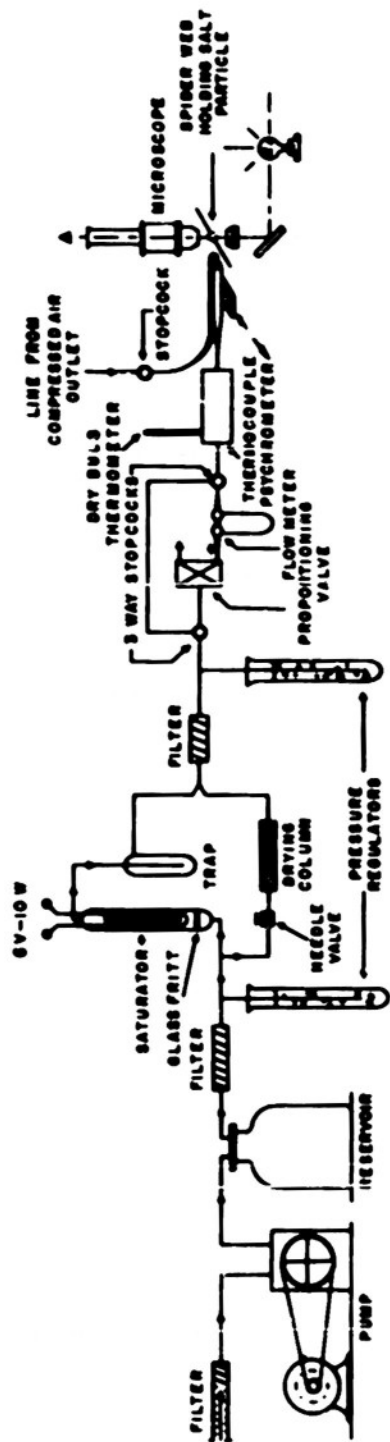


Fig. 3. Sea salt particle growth curves calculated by equation (20) at various fractional humidities and dry bulb temperature of 25°C. Multiplication of σ , the scaled radius, by the cube root of nucleus mass, and τ , the scaled time, by the nucleus mass raised to the 2/3 power, converts the coordinates to droplet radius in microns and time in seconds.



- ① DRY BULB THERMOMETER and THERMOCOUPLE JUNCTION
- ② DRY BULB JET and CHAMBER
- ③ WET BULB JUNCTION TOWNS WITH THREAD
- ④ LEADS TO LAMP AMPLIFIER and SPEEDOMAX RECORDER
- ⑤ MERCURY STOPPER FOR SATURATING WICK
- ⑥ DRY AIR TUBE
- ⑦ HUMID AIR TUBE
- ⑧ SLIDING SEED TO CHANGE DROP FROM DRY TO HUMID AIR
- ⑨ SPIDER WEB and SALT PARTICLE
- ⑩ 10X MICROSCOPE OBJECTIVE
- ⑪ 10X OBJECTIVE
- ⑫ RETICULE
- ⑬ EYEPIECE

Fig. 4. A schematic diagram of the growth rate apparatus, including a detailed drawing of the psychrometer and microscope.

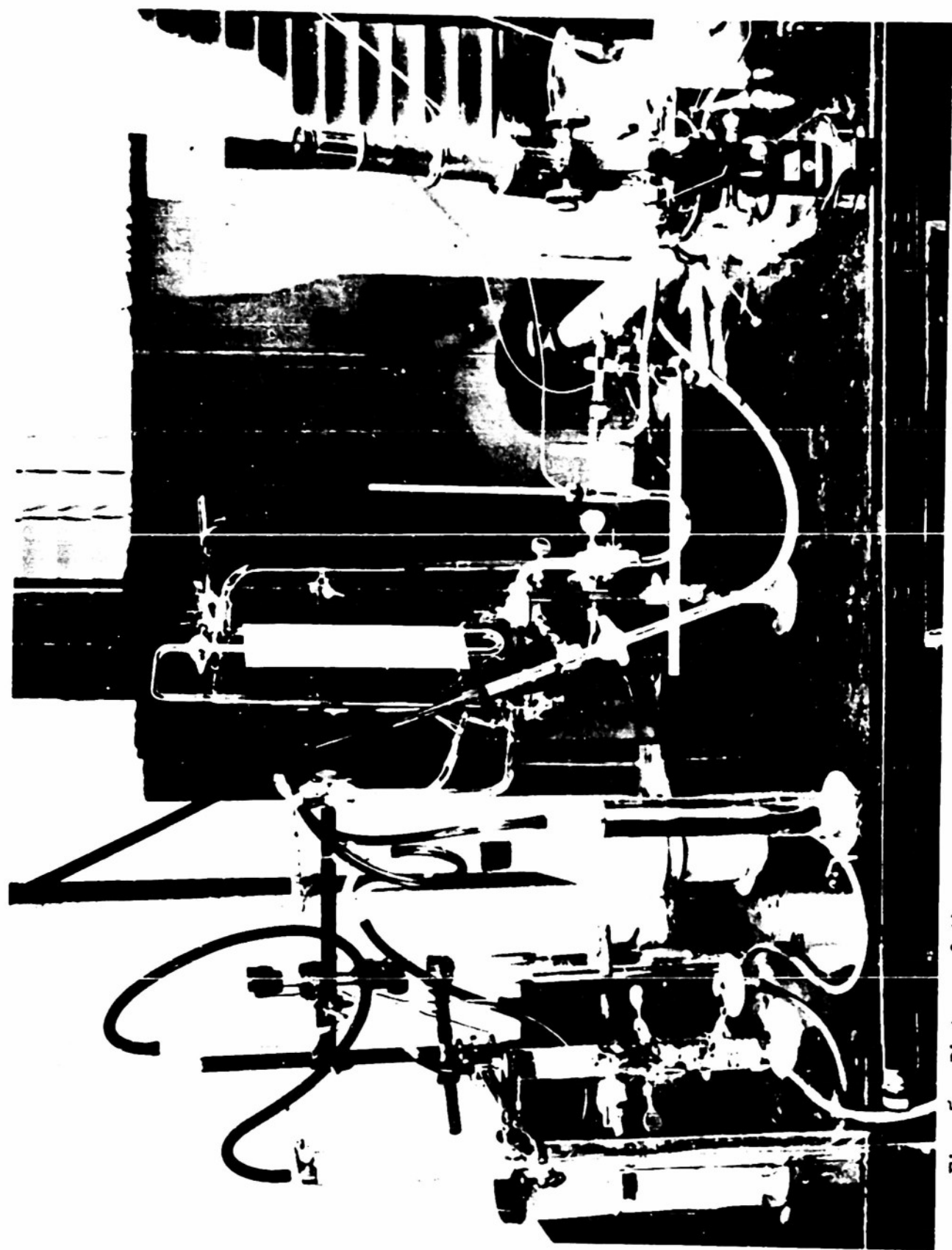


Fig. 5. Picture of the apparatus, showing the arrangement of the various components of the system. Air enters from the Pressovac pump through the rubber tube at the lower left corner of the picture.

III Measurement of growth rates

To test the validity of the derived growth equations, it was necessary to observe the size of a growing sea salt particle as a function of time under known conditions. The principal condition was that the relative humidity be changed nearly discontinuously from a value below 78% where the nucleus is essentially a dry crystal to a constant measurable value above 78%, which will cause growth. Also, it was necessary that a constant temperature and air flow be maintained during growth.

A. Apparatus

A schematic diagram, and pictures of an apparatus which fulfilled these conditions, are presented in Figs. 4 and 5. The principal components were: (1) a system to provide a continuous flow of air of constant humidity; (2) measuring units consisting of a flowmeter and psychrometer; (3) a microscope and special stage to permit observation of the growing particle.

(1) Basically the humidity system was of the divided flow type outlined by Wexler and Brombacher (1951). The desired humidity was obtained by recombination of a divided air stream, one portion of which was saturated, and the other dessicated. The humidity was controlled by adjustment of the relative flow in the two branches by means of a needle valve in the dry branch.

A pumped stream of room air, which had been filtered and dropped to a constant pressure by the first water bubbler, was divided. One part passed through a coarse sintered glass

fritt and rose as small bubbles through a heated column of water, thus becoming saturated with water vapor. Any condensed or sprayed water was removed by a trap attached to the saturator. The other portion of the stream passed through the regulating needle valve and a silica gel drying tower. A small glass wool filter insured mixing of the recombined air stream as well as removal of any silica dust. A second bubbler protected the system from variations in downstream flow which would upset the flow balance between the wet and dry branches.

(2) After passing through the generating system the air stream normally flowed through a proportioning valve and flowmeter. The proportioning valve was essentially two needle valves coupled together so that closure of one resulted in opening of the other. Incoming air was thus divided, one part being exhausted into the room, the other being sent on to the flowmeter. The flowmeter consisted simply of a capillary restriction bridged by a manometer filled with butyl sebacate. At high relative humidities the pressure drop across these units prohibited their use, therefore a by-pass was provided.

The construction of the next unit, the psychrometer, is shown in the detail drawing in Figure 4. This and the rest of the apparatus was constructed mainly of glass tubing for the purposes of cleanliness and low heat conduction. The two one millimeter jets were necessary to insure a high velocity of a flow past the wet and dry thermocouple junctions. The copper-constantan thermocouple was similar to those described by Powell (1936) and had essentially the same response charac-

teristics. An important construction detail was the use of silver solder at the junctions to eliminate stray electrical effects caused by hydrolysis or ordinary solders. The wick was formed by wrapping the wet junction and one centimeter of each lead with #60 cotton thread. The thermocouple leads were connected to a Leeds & Northrup D. C. Amplifier and Speedomax recorder (not shown in Figure 4). The amplification was such that 100 microvolts input (81% relative humidity at 25°C) gave a full scale deflection.

The psychrometer and the tubes leading to and from it were normally protected against radiation heating by a thick covering of glass wool as well as an aluminum foil shield between it and the observer. The outlet tube led directly to the microscope stage through a short length of rubber tubing.

(3) Figure 4 also includes a detail drawing of the microscope and the humidity switching mechanism mounted on the stage. The significant construction details were as follows: The altered lens system was necessary to allow a magnification of 625 diameters with a 1 centimeter working distance. The real image formed by the 6X primary objective was viewed and magnified by a fixed, shortened microscope consisting of a 10X objective and 15X eyepiece. The droplet diameter was read on a calibrated eyepiece reticule.

The spider web carrying the experimental particle was located at the tips of the brass holding rods. Dessens (1947) procedure for obtaining and mounting spider webs was employed. The salt particles were obtained by passing the

webs and holder through mist formed by atomizing Woods Hole sea water.

Tapered glass tubes, (one connected to the humid air supply, the other to a compressed air line), were mounted on a slide which served as the humidity switching system. The extreme positions of the slide were fixed by set screws so that the salt particle under observation was bathed either by air of a known high humidity or by relatively dry air of 30 to 40 percent relative humidity. The size of the tubes (1 centimeter inside diameter) in relation to the droplet size (.001 - .01 cm) and the proximity of the droplet to the mouth of the tube (approximately .08 cm) insured that the particle was surrounded by undiluted air flowing from either tube almost immediately following a shift of tubes. The slide and the stage adjustments were provided with long handles to remove local heating effects. For the same reason, light from the microscope lamp was filtered through a dilute solution of copper sulfate.

Prior to the development of this humidity switcher, a number of measurements were made with enclosed tubes containing the droplet. The humidity shift was obtained by flushing out the dry air initially present in the tube with a known flow of moist air. However, simple experiments with ink flushing out a plug of water showed that the time necessary for nearly complete replacement was of the same magnitude as

the growth time.¹

The time measurement was performed by means of the scale marking pen of the Speedomax recorder; the initial mark indicated the humidity shift at the start of the run, and succeeding marks corresponded to diameter readings. A chart speed of 1 inch per minute permitted time estimation to the nearest second.

B. Calibration of Flowmeter and Psychrometer

A displacement method was used to calibrate the flowmeter. The time required to displace three liters of water by air at atmospheric pressure was measured. The rates of flow thus obtained were plotted against the mean of the flowmeter readings taken during each displacement, providing a calibration curve of the meter against flow in cubic centimeters per second. It was found that the average deviation of the mean flowmeter reading was 0.3 percent over the range from 2 to 18 cc/sec⁻¹.

The usual gravimetric method was used for calibration of the psychrometer. Three tubes, the first containing silica gel, and the others pumice impregnated with sulfuric acid, were used to absorb the vapor contained in the air discharged by the psychrometer, and the weight change over a period of 20 minutes was determined. During the absorption,

¹Woodcock (1952) reports some preliminary growth rates measured in a chamber which was flushed with moist air. The overly long growth times he obtained were probably caused by the inability of obtaining a discontinuous humidity change by such methods.

the temperature, humidity, flow, and atmospheric pressure were recorded and averages obtained. The relative humidity was obtained directly from the ratio of weight of absorbed water per unit volume of air to that contained in a unit volume of saturated air. Comparison of the calculated values with those obtained from the psychrometer indicate that the latter were approximately 0.5% low.

C. Experimental Procedure

The derived growth equations predict that the rate of growth should be dependent upon three variables, mass of salt, humidity, and temperature. A fourth possible variable is the rate of air flow past the growing particle, which was ignored in the development of the growth equation. The design of the apparatus permitted the control of three of these, but since room air of fairly constant temperature was pumped through the apparatus, no attempt was made to investigate the temperature dependence. The effect of each variable was investigated independently by keeping the others nearly constant during a series of measurements. Repeated runs were made at low humidities to obtain a sufficient number of diameter measurements.

The growth measurements were started when the apparatus had become stabilized at a given humidity. This was usually achieved within an hour after starting the pump, or within 10 to 20 minutes following a change of needle valve setting. The stability was generally excellent, in that humidity changes of 0.5% in a period of half an hour were

rare, whereas the same psychrometer showed rapid fluctuations of 10 to 20 % when exposed to room air.

The procedure for an individual run was as follows:

- (1) The initial diameter, temperature, and flow were recorded.
- (2) The slide was shifted, changing the droplet environment from dry to humid air, and a time mark made simultaneously.
- (3) Observations of the changing droplet diameter were made as rapidly as possible, with a corresponding time mark for each recorded diameter.
- (4) The diameter measurements were continued until it was certain that an equilibrium diameter had been reached.
- (5) The temperature and flow were recorded at intervals during the run.
- (6) The humidity and flow were obtained respectively from the psychrometric chart and calibration curve, and the mass of salt was calculated from the equilibrium diameter and humidity by the isopiestic method outlined by Woodcock (1949).

After completion of a series of runs on a given salt particle, the data were averaged to obtain the best possible experimental value of mass of the particle, and this mean was used to scale the diameter and time measurements in accordance with equations (12) and (13).

IV Comparison of experimental results

The experimental results are tabulated in appendix 2, and plotted in Figures 6 through 9. A logarithmic time scale is used in these Figures to spread out scaled time values in the early stages of growth.

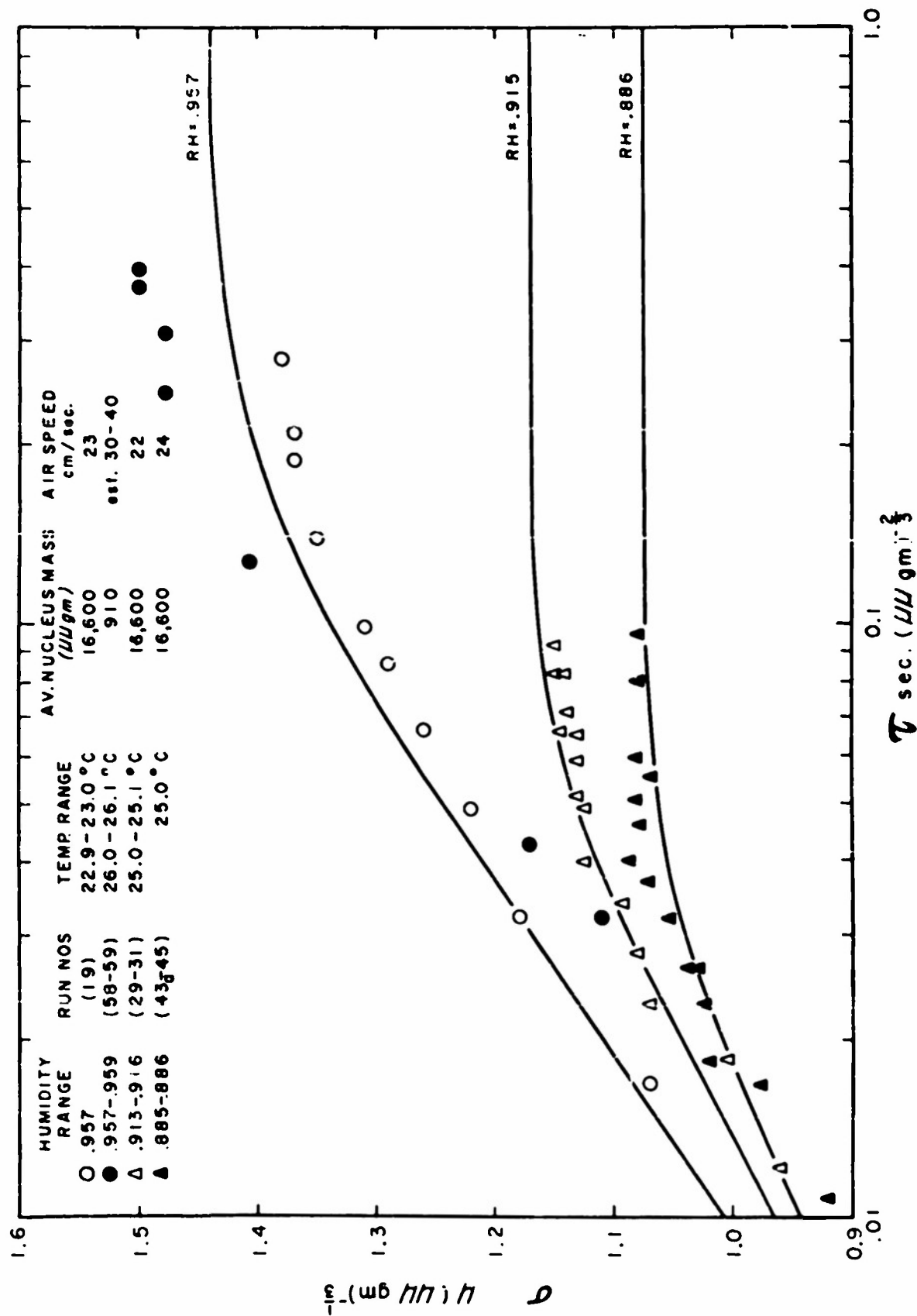


Fig. 6. Comparison of experimental data with growth curves interpolated from Fig. 3. The legends following each symbol relate the humidity range, the sequence numbers of the runs, the dry bulb temperature range, the average nucleus mass, and the air speed during the measurement.

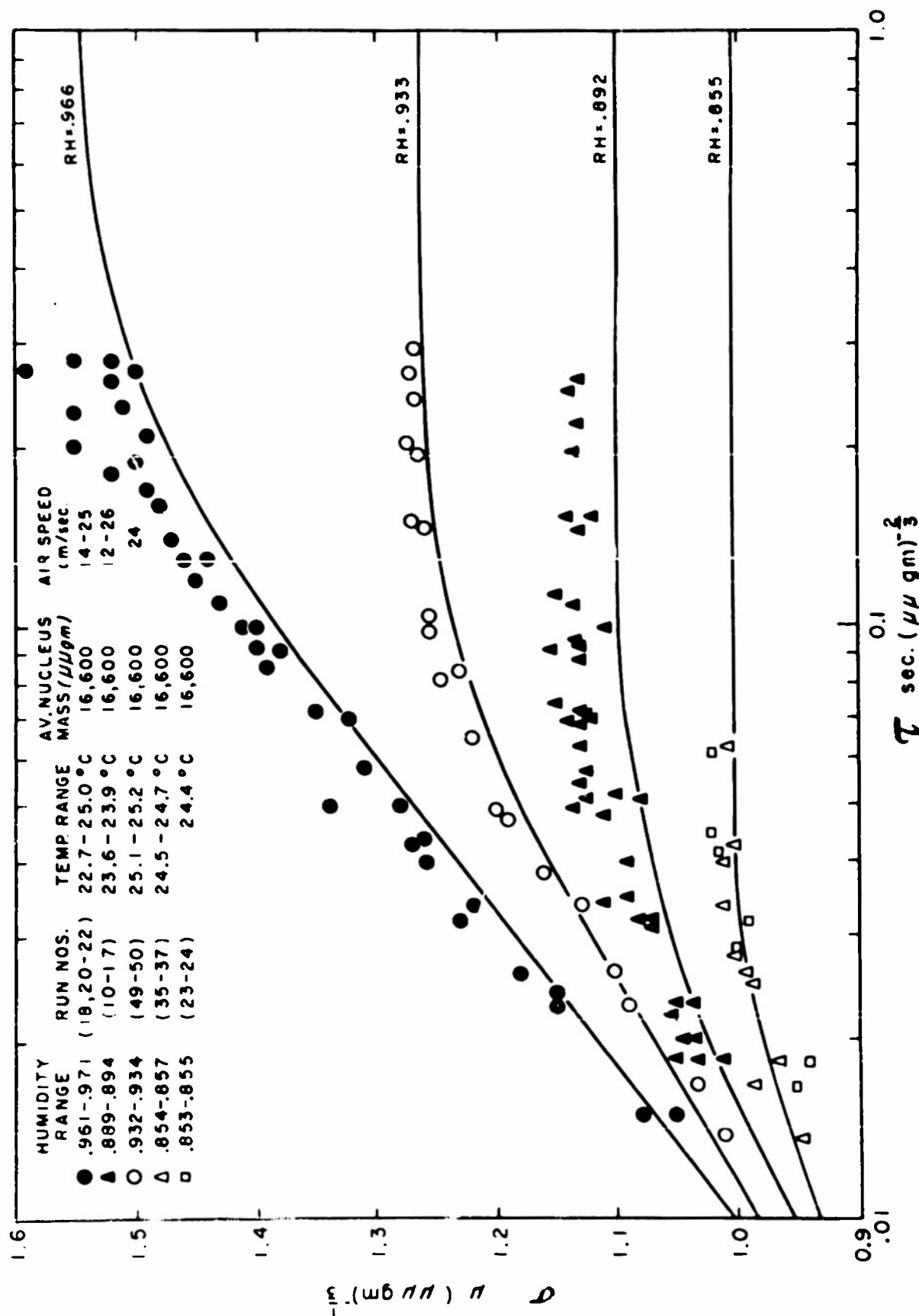


Fig. 7. Comparison of experimental data with growth curves interpolated from Fig. 3. The legends following each symbol relate the humidity range, the sequence numbers of the runs, the dry bulb temperature range, the average nucleus mass, and the air speed during the measurement.

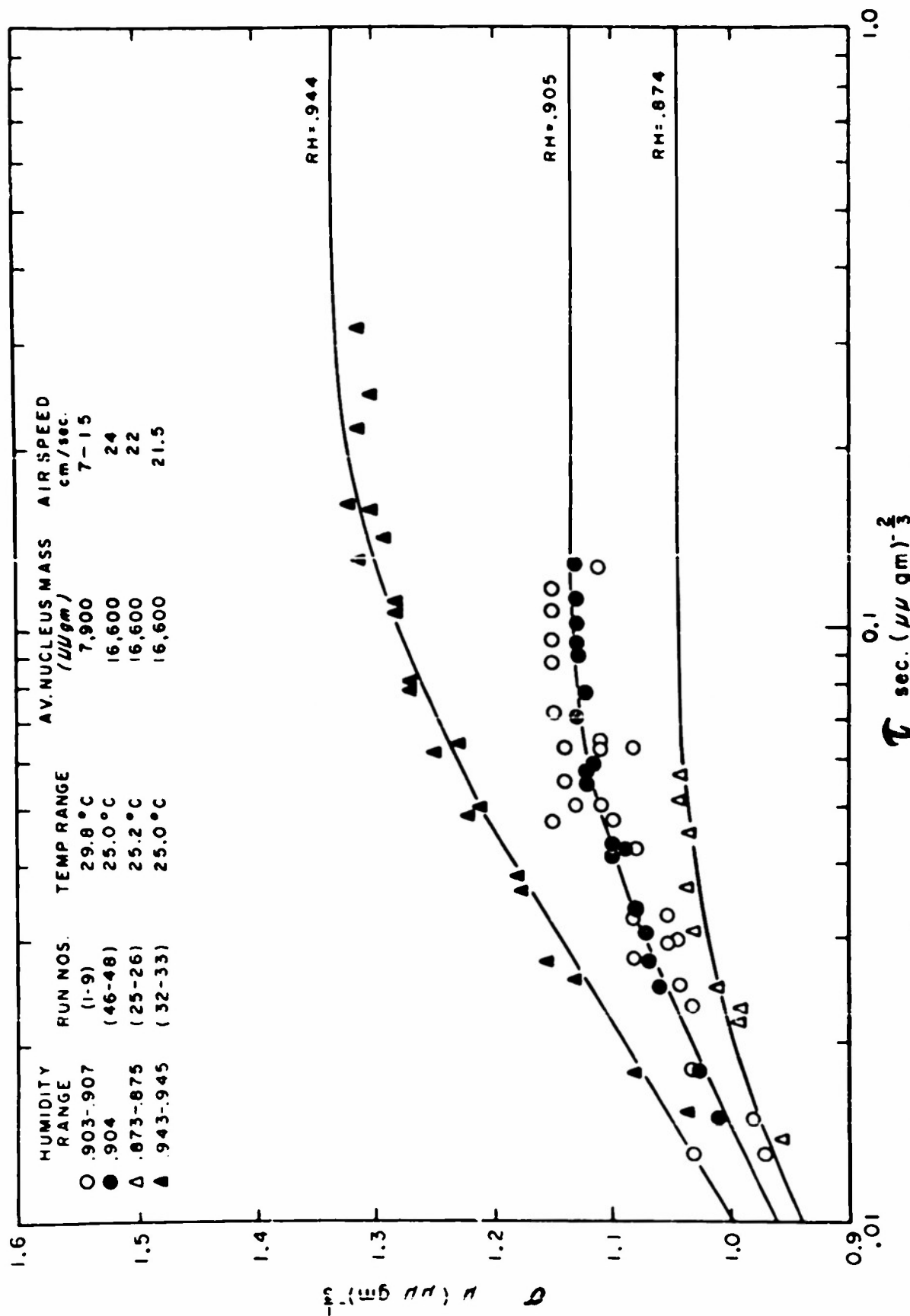
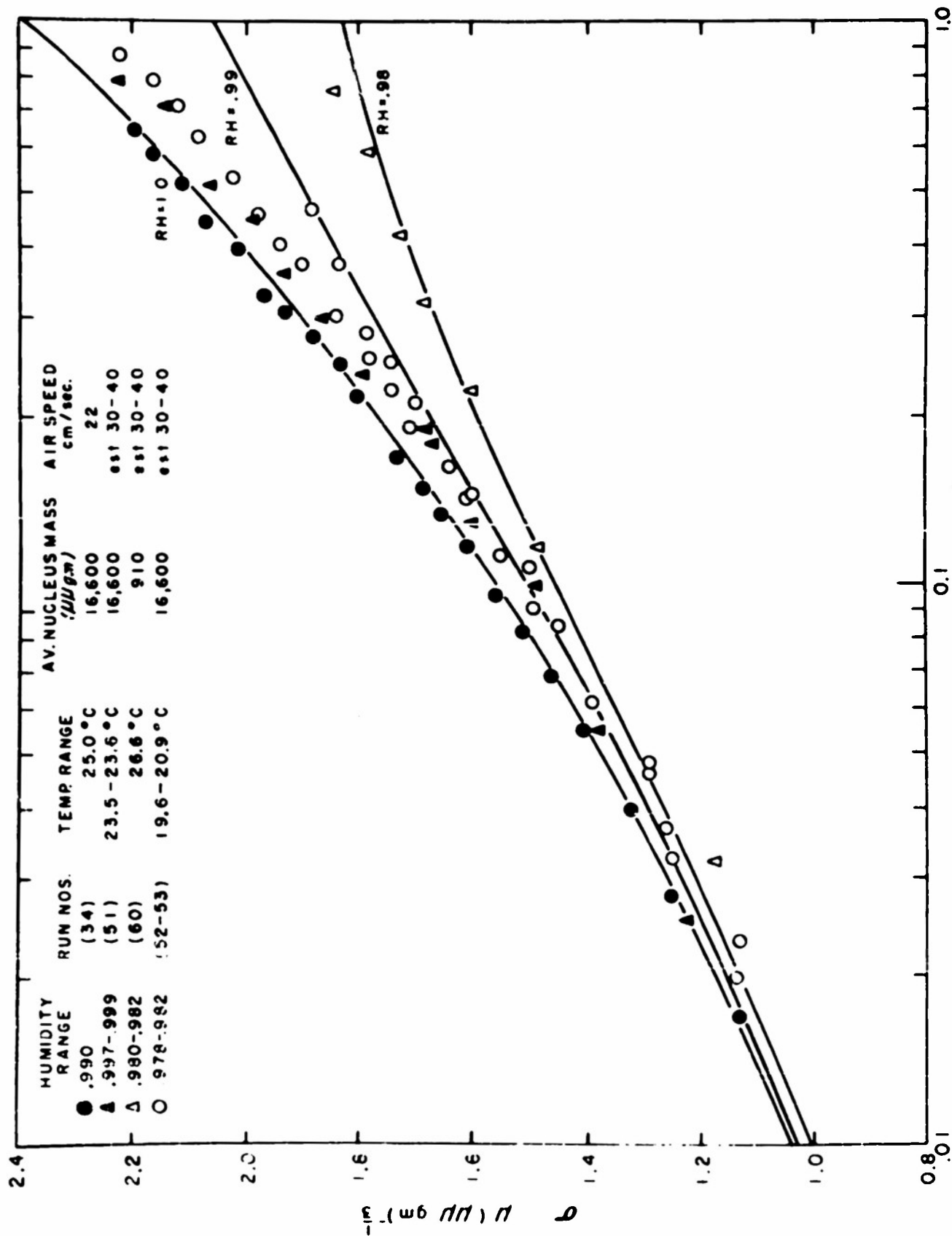


Fig. 8. Comparison of experimental data with growth curves interpolated from Fig. 3. The legends following each symbol relate the humidity range, the sequence numbers of the runs, the dry bulb temperature range, the average nucleus mass, and the air speed during the measurement.



$\tau_{\text{sec}} (\mu\text{g})^{\frac{2}{3}}$

Fig. 9. Comparison of experimental data with growth curves interpolated from Fig. 3. The legends following each symbol relate the humidity range, the sequence numbers of the runs, the dry bulb temperature range, the average nucleus mass, and the air speed during the measurement.

Runs 1-9, represented by the open circles of Fig. 8, were made with a 7,900 micromicrogram particle at rates of air flow between 7 and 15 cm/sec. Similarly, runs 10-17 were performed with a 16,600 micromicrogram particle at flows between 12 and 26 cm/sec.

The same 16,600 micromicrogram salt particles was used for runs 18 through 53.

The final series of runs, numbers 54 through 60, were performed with a considerably smaller 910 micromicrogram particle.

The theoretical curves of Figs. 6-9 were obtained by graphical interpolation between those of Fig. 3.

Before discussion of the comparison between experiment and theory, it is necessary to estimate the effects of observational errors upon the data. The scatter of the individual diameter measurements was caused by the difficulty in estimation of the changing diameter of the droplet at a given instant of time. The diameters were read on a reticule with a calibration of 2.4 microns per scale unit. Thus, if either edge is estimated to $\pm .2$ of a scale unit, the diameter is good to $\pm .1$ micron, which amounts to $\pm .04$ sigma units for the largest particle observed (16,600 micromicrograms). For a 1000 micromicrogram particle, the error of an individual diameter measurement increases to $\pm .1 \mu (\mu \mu \text{ gm})^{-1/3}$.

The psychrometer introduces another significant source of error. The calibration indicates that the precision of a humidity measurement is $\pm 0.5\%$. The effect of this may

be estimated directly from Fig. 3 by interpolation between the growth curves. Errors in σ of 2 to 6% are possible, depending upon the humidity and stage of growth. It should be noted in Fig. 9 that the data tends to fall near the saturation curve, although the measured humidity is from 1 to 2% less than saturation. These deviations are not surprising since random heating, slight pressure drops, and condensation on the tubing walls make the attainment and maintenance of these high humidities difficult.

In view of the possible errors, it is apparent that the agreement between experiment and theory is generally good. All the deviations from the computed curves are within, and usually considerably less than, the estimated limit of experimental error. Therefore it is concluded that the approximate growth equation (20) satisfactorily describes the growth of saline particles in a humid atmosphere. The mathematical approximations, neglect of heat storage effects, and use of macroscopic diffusion and heat conduction coefficients are valid. However, the 3 to 14% difference between the equilibrium scaled radii of equation (21) and those computed by Wright's (1936) formula indicate that the use of a Raoult's law vapor pressure dependence in earlier work led to significant error.

The effect of ventilation was investigated in two series, runs 1-9 and 10-17. In both series separate runs were made with the same particle and humidity, but with different rates of flow. There is no observable variation

in growth rate over the range of flows measured (7 to 26 cm. sec⁻¹). Below the velocity of 7 cm. sec⁻¹ there were indications of a slower rate of growth. However, it is believed that this was due principally to the increased time necessary for changing the droplet surroundings. Similarly, this effect prohibited growth measurements on droplets of mass less than 1000 micromicrograms, because of their very short overall growth time.

When the bypass of the flowmeter was used for runs at high humidities, the velocity of air flow was estimated to be between 30 and 40 cm. sec⁻¹. No velocity effect was apparent in the comparison between the data from these runs and the theoretical curves.

The observed absence of a ventilation effect agrees with the results obtained by Kinzer and Gunn (1951). They found that the rate of evaporation of drops falling at terminal velocities less than 1/2 meter per second was also predicted by a static diffusion equation.

V Growth under variable humidity conditions.

Now that the formulations derived in Section II have been shown to be valid, it is of interest to apply them to problems of meteorological significance. The essential agreement between the foregoing development and that of Powell (1949) and Squires (1952), and the excellent treatment given by these authors for conditions prevailing within a cloud, preclude any great improvement by rediscussion of that phase of the problem. However, an estimate of the size of droplets

in sub-cloud air would be of use in understanding the role of salt nuclei in rain formation and visibility.

As an illustration of the use of the growth equation (20), the equation was applied to the arbitrary situation of a particle rising at a steady rate from an atmosphere approximating that near the sea surface in the trade-wind areas ($T_1 = 25^\circ\text{C}$, $H = .65$). It is also assumed that the temperature falls 1 degree centigrade per 100 meters, corresponding to a dry adiabatic expansion. Since the growth equation is primarily humidity dependent, and only slightly temperature dependent, the initial temperature and humidity conditions are not critical, save in that the humidity be less than the solution point, $H = .78$. The use of a dry adiabatic lapse rate makes the rate of rise nearly proportional to the time rate of change of humidity, which is the parameter utilized in equation (20).

By use of the specified conditions, equation (20) becomes:

$$\sigma \frac{d\sigma}{dH} = \frac{2 \times 10^3 A}{V m_0^{2/3}} \ln \frac{1 - .146 \sigma^{-3.35}}{H} \quad (24)$$

Upon choice of a suitable updraft (1 meter per second) and nucleus size, equation (24) may be integrated to yield growth curves. Because of the dependence of this equation upon individual nucleus sizes, and the temperature dependence of A, a crude method of integration was utilized to reduce the computation time. After initially choosing reasonable values of scaled radius and humidity, a slope $\frac{d\sigma}{dH}$ was obtained by equation (24). This slope, when expressed in the form of finite

increments, provided new values of σ and H , which in turn allowed the computation of a new slope. Iteration of this process was used to construct the curves of Fig. 10. The increments in σ and H were kept small enough so that a second approximation of any individual slope was unnecessary. After a sufficient number of curves at a 1 meter per second updraft had been obtained, curves at other updrafts were obtained by a simple shift of variables in (24). Identical growth curves will be obtained for two different particles rising at different rates if $VM_s^{2/3}$ is the same in both cases. For example, the growth curve of a 1000 micromicrogram particle rising at 1 meter per second will be the same as that of a 2828 micromicrogram particle rising at 1/2 meter per second.

Fig. 11 shows the droplet size attained by particles of the indicated masses at the saturation level (cloud base) following a steady rise at the indicated rates. It is apparent that the rate of rise does not greatly affect the droplet size attained by the more numerous small particles. Consequently, it is to be expected that most of the 1 meter per second curves of Figs. 10 and 11 would apply under normal atmospheric conditions, even with erratic updrafts and variable initial conditions.

The apparent growth of all particles of mass less than 50 micromicrograms to a radius of about 5 microns coincides with Howell's findings that very small nuclei generate a narrow spectrum of droplet sizes. This is presumed to be

caused by rapid growth of these particles to an extremely dilute droplet, the growth of which is thenceforth almost independent of the mass of the original nucleus.

In Fig. 11 a radius of 15 microns or more is attained by particles of mass greater than 400 micromicrograms, which are present in trade-wind regions in numbers comparable to raindrops (500 - 5000 per cubic meter, Woodcock, 1952). These particles are of sufficient size to grow at an appreciable rate by accretion of smaller droplets. The accretional rate of growth, as estimated by Houghton's (1950) curve, is approximately a tenth to a hundredth of the condensational rate for nuclei of the sizes indicated by Fig. 11. However, the accretional rate rapidly increases, while the condensational rate decreases with increasing droplet size. This would make it probable that condensational growth within the cloud layer is of secondary importance to the process of accretional growth in the formation of raindrops upon salt nuclei.

VI Acknowledgement

The authors are indebted to Mr. Alfred Woodcock for his helpful advice on the experimental portions of this work and for the original impetus to undertake this study. We also wish to thank Mrs. Mary C. Thayer, who performed the computations upon the original data.

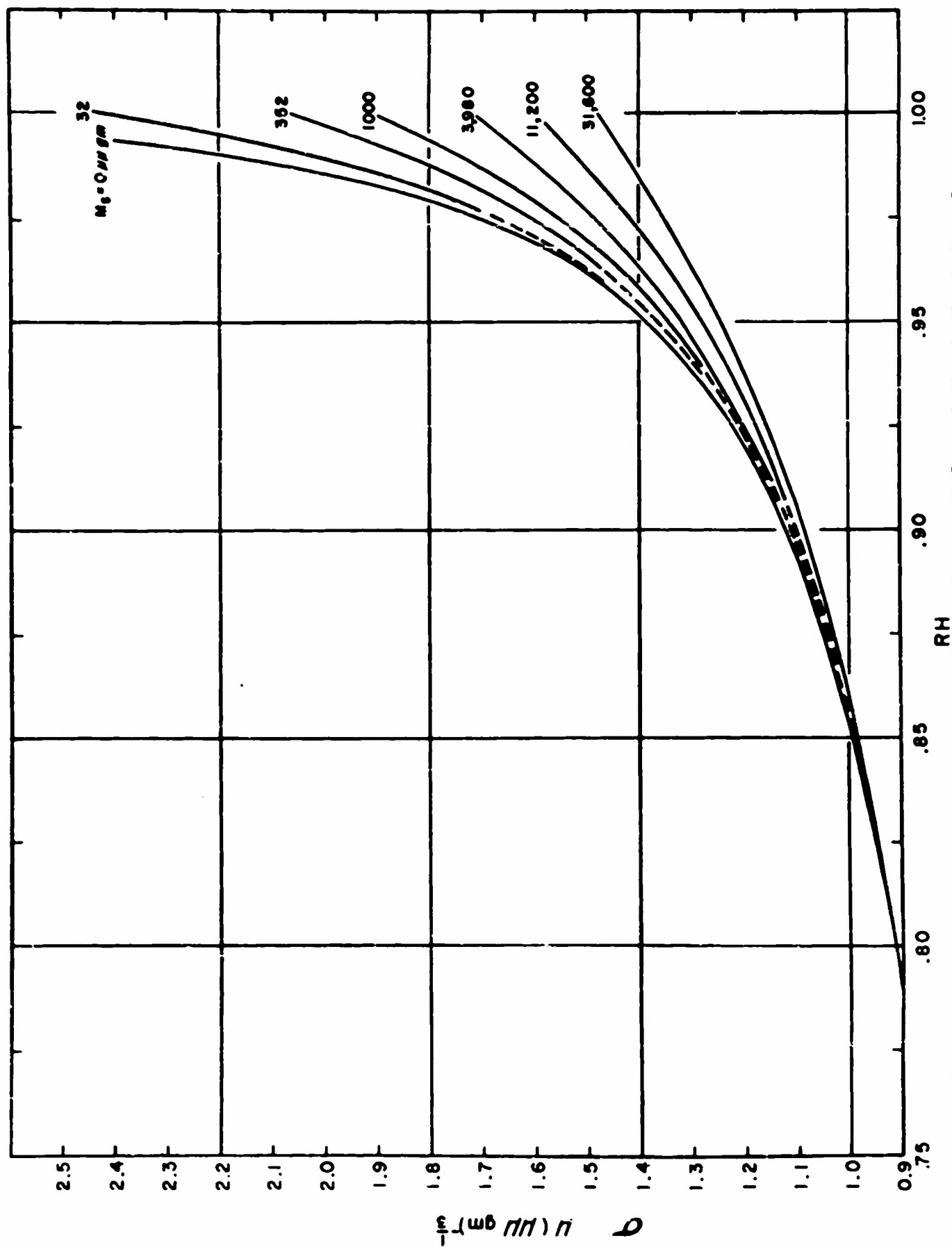


Fig. 10. Variation of sigma with humidity for particles of the indicated nucleus masses rising at 1 meter per second from a level of 25°C and 65% relative humidity. The temperature decrease is assumed to be 1°C per 100 meters.

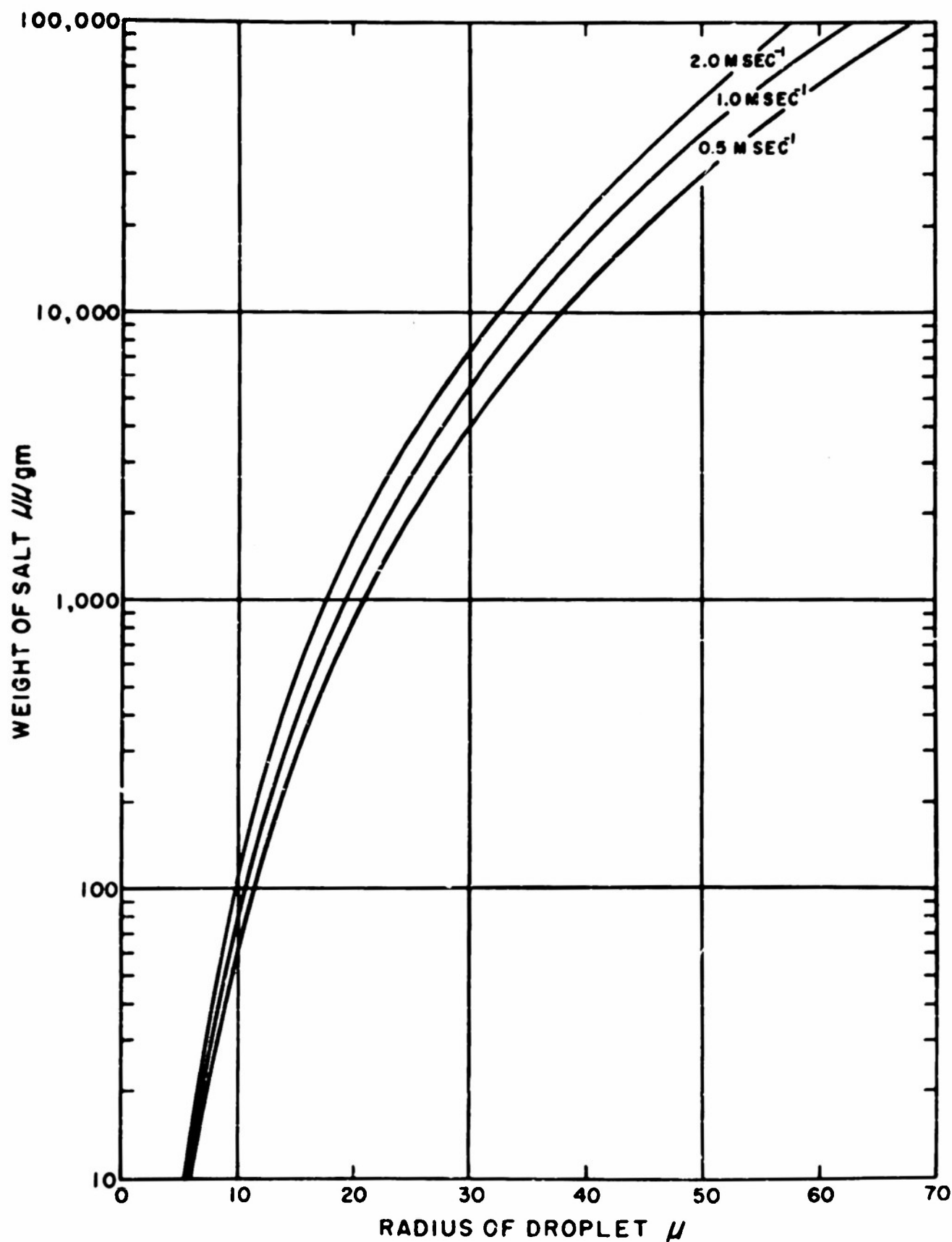


Fig. 11. The calculated radius of sea salt droplets at cloud base ($H = 1.0$) presented as a function of nucleus mass and rate of rise. The initial conditions are the same as those of the preceding Figure.

References.

- Arons, A. B. and C. F. Kientzler, 1953: Vapor pressure of sea salt solutions. *J. Mar. Res.* (in press)
- Best, A. C., 1951: The size of cloud drops in layer type cloud. *Quart. J. r. meteor. Soc.*, 77, 241-248.
- _____, 1953: Condensation nuclei and the development of radiation fog. *Quart. J. r. meteor. Soc.*, 79, 41-56.
- Dessans, H., 1947: Brume et noyaux de condensation. *Ann. Geophys.*, 2, 68-85.
- Houghton, H. G., 1950: A preliminary quantitative analysis of precipitation mechanisms. *J. Meteor.*, 7, 363-369.
- Howell, W. E., 1949: The growth of cloud drops in uniformly cooled air. *J. Meteor.*, 6, 134-149.
- Higashi, K., K. Nakamura, and R. Hara, 1931: The specific gravities and the vapor pressure of the concentrated sea water at 0-175°C. *J. Soc. Chem. Ind. Japan*, 34; 166-172. (Abstr. 72B).
- Kinzer, G. D., and Ross Gunn, 1951: The evaporation, temperature, and thermal relaxation-time of freely falling raindrops. *J. Meteor.*, 8, 71-83.
- Kraus, E. B., and Betty Smith, 1949: Theoretical aspects of cloud drop distributions. *Aust. J. Sci. Res.*, A2, 376-388.
- Langmuir, I., 1944: Super-cooled water droplets in rising currents of cold saturated air. General Electric Co., Schenectady, 150 pp.
- McDonald, J. E. 1953: Erroneous cloud-physics applications of Raoult's law. *J. Meteor.*, 10, 68-70.
- Powell, R. W., 1936: The use of thermocouples for psychrometric purposes. *Proc. Phys. Soc. (London)*, 48, 406-414.
- Squires, P., 1952: The growth of cloud drops by condensation. *Aust. J. Sci. Res.*, A5, 59-86.
- Thompson, T. G., and R. T. Robinson, 1932: Chemistry of the sea. Physics of the Earth, 5, Oceanography, Bull. Nat. Res. Council, No. 85, 187-193.

- Wexler, A., and W. G. Brombacher, 1951: Methods of measuring humidity and testing hygrometers. Nat. Bur. Stand. Circular 512, 18 pp.
- Woodcock, A. H., and Mary M. Gifford, 1949: Sampling of atmospheric sea-salt nuclei over the ocean. J. Mar. Res., 8, 177-197.
- Woodcock, A. H., 1952: Atmospheric salt particles and raindrops. J. Meteor., 9, 200-212.
- Wright, H. L., 1936: The size of atmospheric nuclei. Proc. Phys. Soc. (London), 48, 675-689.

APPENDIX I

Table of Symbols and Constants

q	=	quantity of water vapor (gm)
Q	=	quantity of heat (cal.)
$\left[\frac{d\rho}{dr}\right]$	=	vapor density gradient (gm cm ⁻⁴)
$\left[\frac{dT}{dr}\right]$	=	temperature gradient (deg Kelvin cm ⁻¹)
R'	=	radial distance (cm)
D	=	diffusion coefficient of water vapor in air (cm ² sec ⁻¹)
k	=	heat conduction coefficient of moist air cal cm ⁻¹ sec ⁻¹ deg ⁻¹
C_p	=	specific heat of water at constant pressure (cal gm ⁻¹ deg ⁻¹)
T_1	=	temperature of surrounding air (deg)
T	=	temperature of droplet (deg)
ρ_1	=	vapor density of surrounding air (gm cm ⁻³)
ρ	=	vapor density of droplet at temperature of droplet (gm cm ⁻³)
p_1	=	vapor pressure of surrounding air (mm Hg)
p	=	vapor pressure of droplet of temperature of drop- let (mm Hg)
p_2	=	vapor pressure of droplet at temperature of sur- rounding air (mm Hg)
t	=	time (seconds)
m	=	mass of droplet (gm)
m_s	=	mass of salt particle (gm)

m_w = Mass of water in droplet (gm)

r = radius of droplet (cm)

ρ_s = density of solution comprising droplet (gm cm⁻³)

L = latent heat of condensation of water vapor (cal gm⁻¹)

R = gas constant (cal mole⁻¹ deg⁻¹ or cm³(mm Hg) mole⁻¹ deg⁻¹)

M = mole weight of water (gm mole⁻¹)

σ = scaled radius (cm gm^{-1/3} or $\mu\mu\text{gm}$)^{-1/3}

τ = scaled time (sec gm^{-2/3} or sec ($\mu\mu\text{gm}$)^{-2/3})

Δp = vapor pressure lowering (mm Hg)

H = fractional relative humidity

p_0 = saturation vapor pressure (mm Hg)

σ_{eq} = equilibrium scaled radius

τ_0 = scaled time for growth from dry crystalline mass
to droplet of saturated solution

V = rate of rise of particle (meters sec⁻¹)

APPENDIX II

Experimental data

$m_s = 7,900$ ~~mm~~ grams average

RUN	RH	T	V
1	.909	29.0°C	14.9 cm sec ⁻¹
	$\frac{d = 2r}{\mu}$	$\mu (\frac{\sigma}{\mu \mu \text{ gm}})^{1/2}$	$\frac{t}{\text{sec}}$
			sec $(\frac{\sigma}{\mu \mu \text{ gm}})^{1/2}$
	33.6	.84	3
	40.8	1.03	9
	45.6	1.15	19
2	.909	29.0°C	14.9 cm sec ⁻¹
	40.8	1.03	5
	43.2	1.08	11
	45.4	1.14	22
	45.6	1.15	43
3	.909	29.0°C	14.9 cm sec ⁻¹
	40.8	1.03	7
	43.2	1.08	14
	45.4	1.14	25
	45.6	1.15	37
4	.909	29.0°C	12.1 cm sec ⁻¹
	38.4	0.97	5
	43.2	1.08	11
	44.4	1.11	20
	45.6	1.15	29
5	.908	29.0°C	12.1 cm sec ⁻¹
	38.4	0.97	5
	41.5	1.04	12
	43.7	1.10	19
	44.4	1.11	25
	45.6	1.15	35
6	.907	29.0°C	8.3 cm sec ⁻¹
	38.4	0.97	5
	42.0	1.05	12
	44.4	1.11	20
	45.6	1.15	35

RUN 7 RH = .907 T = 29.0°C V = 8.3 cm sec⁻¹

<u>d = 2r</u>	<u>σ</u>	<u>t</u>	<u>τ</u>
38.9	0.98	6	.015
43.2	1.08	13	.033
45.1	1.13	20	.051
45.6	1.15	46	.116

RUN 8 RH = .903 T = 29.0°C V = 6.9 cm sec⁻¹

38.4	0.97	5	.013
42.0	1.05	13	.033
43.2	1.08	25	.063
44.4	1.11	50	.126

RUN 9 RH = .905 T = 29.0°C V = 6.9 cm sec⁻¹

34.8	0.87	3	.0076
41.3	1.04	10	.025
43.2	1.08	17	.043
44.4	1.11	26	.066

m = 16,600 μμ grams average

RUN 10 RH = .889 T = 23.6-23.7°C V = 26.0 cm sec⁻¹

48.0	.94	6	.0092
52.8	1.035	12	.0185
54.7	1.070	20	.031
56.9	1.11	31	.048
57.4	1.125	46	.071
57.6	1.13	60	.092
57.6	1.13	94	.145
57.9	1.135	129	.199
58.1	1.14	161	.25

RUN 11 RH = .889 T = 23.7-23.8°C V = 26.0 cm sec⁻¹

45.6	.90	6	.0092
53.8	1.055	14	.022
55.5	1.09	26	.040
57.4	1.125	37	.057
57.6	1.13	44	.068
57.9	1.135	62	.095
58.1	1.14	100	.154

RUN 12 RH = .889-.890 T = 23.8-23.9°C V = 23.5 cm sec⁻¹

<u>d = 2r</u>	<u>σ</u>	<u>t</u>	<u>τ</u>
40.8	.80	3	.0046
52.8	1.035	13	.020
55.2	1.08	21	.032
57.6	1.13	35	.054
57.6	1.13	47	.072
57.9	1.135	70	.108
57.9	1.135	94	.145
57.6	1.13	142	.22
57.6	1.13	171	.26

RUN 13 RH = .890 T = 23.9°C V = 23.5 cm sec⁻¹

40.8	.80	3	.0046
51.6	1.01	12	.0185
54.7	1.07	21	.032
55.2	1.08	33	.051
56.5	1.11	64	.099
57.1	1.12	98	.151
57.6	1.13	140	.22

RUN 14 RH = .890 T = 23.9°C V = 21.1 cm sec⁻¹

43.2	.85	4	.0062
53.5	1.05	15	.023
55.5	1.09	23	.035
57.4	1.125	33	.051
57.6	1.13	41	.063

RUN 15 RH = .890 T = 23.9°C V = 17.9 cm sec⁻¹

44.5	.87	5	.0077
52.8	1.035	15	.023
55.2	1.08	21	.032
56.2	1.10	34	.052
57.1	1.12	45	.069
57.6	1.13	57	.088

RUN 16 RH = .891 T = 23.9°C V = 15.9 cm sec⁻¹

46.8	.92	5	.0077
53.5	1.05	12	.0185
56.5	1.11	22	.034
57.6	1.13	35	.054
58.4	1.14	45	.069
58.8	1.15	73	.112

RUN 17 RH = .893 T = 23.8°C V = 11.9 cm sec⁻¹

<u>d = 2r</u>	<u>σ</u>	<u>t</u>	<u>τ</u>
48.0	.94	6	.0092
53.3	1.045	13	.020
57.1	1.12	22	.034
57.9	1.135	32	.049
58.8	1.15	48	.074
59.0	1.155	59	.091

RUN 18 RH = .961-.964 T = 22.7°C V = 23.4 cm sec⁻¹

43.2	.84	4	.0061
59.3	1.15	15	.023
62.9	1.23	21	.032
65.3	1.27	28	.043
67.2	1.31	38	.058
71.0	1.39	56	.086
72.0	1.41	66	.10
75.4	1.47	96	.14
76.4	1.49	135	.21
76.8	1.50	176	.27

RUN 19 RH = .957 T = 22.9-23.0°C V = 23.1 cm sec⁻¹

49.2	.96	5	.0076
54.6	1.07	11	.017
60.5	1.18	21	.032
62.6	1.22	32	.049
64.8	1.26	44	.067
66.2	1.29	56	.086
67.2	1.31	68	.10
69.1	1.35	93	.14
70.1	1.37	125	.19
70.1	1.37	140	.21
70.5	1.38	184	.28

RUN 20 RH = .969-.971 T = 24.5°C V = 24.9 cm sec⁻¹

45.6	.91	4	.0061
55.2	1.08	10	.015
60.5	1.18	17	.026
64.8	1.26	26	.040
68.6	1.34	33	.050
72.0	1.40	51	.093
74.0	1.45	80	.12
75.6	1.48	102	.16
76.9	1.50	125	.19
77.3	1.51	154	.235
78.0	1.52	184	.28

RUN 21 RH = .963-.969 T = 24.8-24.9°C V = 19.7 cm sec⁻¹

<u>d = 2r</u>	<u>σ</u>	<u>t</u>	<u>τ</u>
54.0	1.05	10	.015
62.4	1.22	22	.034
65.8	1.28	33	.050
69.2	1.35	47	.072
72.0	1.40	66	.10
73.6	1.44	84	.13
76.0	1.49	113	.17
78.5	1.53	170	.26
79.2	1.55	184	.28

RUN 22 RH = .962-.967 T = 25.0°C V = 13.6 cm sec⁻¹

48.0	.94	5	.0076
59.0	1.15	16	.024
64.4	1.26	29	.044
67.9	1.32	46	.070
70.8	1.38	60	.092
73.2	1.43	72	.11
74.5	1.46	85	.13
78.0	1.52	117	.18
79.2	1.55	130	.20
79.5	1.55	153	.23
81.6	1.59	179	.27

RUN 23 RH = .853-.855 T = 24.4°C V = 23.0 cm sec⁻¹

40.8	.80	5	.0077
48.0	.94	12	.0185
51.1	1.00	19	.029
51.8	1.015	27	.042
52.1	1.02	40	.062

RUN 24 RH = .853 T = 24.4°C V = 23.0 cm sec⁻¹

38.4	.75	5	.0077
48.5	.95	11	.0169
50.6	.99	21	.032
52.1	1.02	29	.045

RUN 25 RH = .873 T = 25.2°C V = 22.0 cm sec⁻¹

45.1	.89	6	.0092
50.4	.99	15	.023
52.8	1.035	24	.037

RUN 26 RH = .875 T = 25.2°C V = 21.9 cm sec⁻¹

<u>d = 2r</u>	<u>σ</u>	<u>t</u>	<u>τ</u>
40.8	.80	4	.0062
50.4	.99	14	.022
52.6	1.030	20	.031
52.8	1.035	30	.046

RUN 27 RH = .875 T = 25.2°C V = 21.9 cm sec⁻¹

36.0	.71	3	.0046
48.7	.955	9	.0138
51.6	1.01	16	.025
52.8	1.035	24	.037
53.0	1.040	37	.057

RUN 28 RH = .875 T = 25.2°C V = 21.9 cm sec⁻¹

45.6	.90	6	.0092
50.6	.99	14	.022
52.8	1.035	24	.037
53.0	1.040	34	.052

RUN 29 RH = .913 T = 25.1°C V = 21.9 cm sec⁻¹

43.2	.85	5	.0077
51.6	1.01	12	.0185
55.2	1.08	18	.028
56.4	1.085	26	.040
57.4	1.125	32	.049
57.6	1.13	41	.063
58.6	1.145	54	.083

RUN 30 RH = .915-.916 T = 25.1°C V = 22.0 cm sec⁻¹

40.8	.80	3	.0046
49.2	.965	8	.0123
54.5	1.07	15	.023
55.7	1.09	22	.034
57.6	1.13	33	.051
58.6	1.145	43	.066
58.8	1.15	54	.083

RUN 31 RH = .916 T = 25.0 V = 22.0 cm sec⁻¹

39.6	.78	2	.0031
52.8	1.035	6	.0092
55.2	1.08	18	.028
57.4	1.125	26	.040
57.6	1.13	38	.059
58.1	1.14	46	.071
58.8	1.15	60	.092

RUN 32 RH = .945 T = 25.0°C V = 21.5 cm sec⁻¹

<u>d = 2r</u>	<u>σ</u>	<u>t</u>	<u>τ</u>
45.6	.90	4	.0062
52.8	1.035	10	.0154
57.6	1.13	17	.026
60.0	1.175	24	.037
61.9	1.21	33	.051
62.9	1.23	42	.065
64.6	1.27	54	.083
65.3	1.28	72	.111
65.8	1.29	93	.143
66.0	1.30	103	.159
66.7	1.31	144	.22
66.2	1.30	163	.25
66.7	1.31	206	.32

RUN 33 RH = .943 T = 25.0°C V = 21.5 cm sec⁻¹

47.3	.93	4	.0062
55.2	1.08	11	.0169
59.0	1.155	18	.028
60.2	1.18	25	.039
62.4	1.22	32	.049
63.6	1.25	41	.063
64.8	1.27	52	.080
65.5	1.28	68	.105
66.7	1.31	85	.131
67.2	1.32	105	.162

RUN 34 RH = .990 T = 25.0°C V = 22.4 cm sec⁻¹

50.4	.99	5	.0008
57.6	1.13	11	.017
63.6	1.25	18	.028
67.2	1.32	26	.040
71.5	1.40	36	.055
74.4	1.46	45	.069
77.3	1.51	54	.083
79.2	1.55	63	.097
82.1	1.61	77	.118
84.0	1.65	88	.135
85.9	1.68	97	.15
88.3	1.73	110	.17
91.7	1.80	143	.22
93.4	1.83	163	.25
96.0	1.88	184	.28
98.4	1.93	202	.31
100.8	1.97	217	.33
102.7	2.01	260	.40

RUN 34
(Contd.)

RH = .990

T = 25.0°C

V = 22.4 cm sec⁻¹

d = 2r

α

t

ε

105.4	2.07	292	.45
107.8	2.11	239	.52
110.2	2.16	385	.59
111.6	2.19	423	.65
112.8	2.21	442	.68
115.2	2.26	484	.745
117.1	2.30	529	.81
118.8	2.33	576	.89
120.0	2.35	610	.94

RUN 35

RH = .856-.857

T = 24.5-24.6°C

V = 24.0 cm sec⁻¹

40.8	.80	4	.0062
49.2	.965	12	.0185
50.4	.99	17	.026
50.9	1.00	28	.043
51.6	1.01	41	.063

RUN 36

RH = .856

T = 24.6°C

V = 24.0 cm sec⁻¹

40.8	.80	3	.0046
48.5	.95	9	.014
50.2	.985	16	.025
51.6	1.01	22	.034

RUN 37

RH = .854-.855

T = 24.6-24.7°C

V = 24.0 cm sec⁻¹

40.8	.80	3	.0046
50.2	.985	11	.017
50.9	1.00	18	.028
51.6	1.01	26	.040

RUN 38

RH = .839

T = 24.7°C

V = 24.0 cm sec⁻¹

38.4	.75	4	.0062
48.0	.94	9	.014
50.6	.99	17	.026

RUN 39

RH = .837

T = 24.7°C

V = 24.0 cm sec⁻¹

40.8	.80	4	.0062
48.0	.94	10	.015
50.2	.98	16	.025
50.6	.99	26	.040

RUN 40 RH = .836-.837 T = 24.8-24.9°C V = 24.0 cm sec⁻¹

<u>d = 2r</u>	<u>σ</u>	<u>t</u>	<u>τ</u>
38.4	.75	4	.0062
46.8	.92	9	.014
49.2	.96	14	.022
50.4	.99	27	.042
50.6	.99	37	.0570

RUN 41 RH = .867 T = 25.0°C V = 24.0 cm sec⁻¹

43.2	.87	6	.0092
50.4	.99	11	.017
51.6	1.01	17	.026
52.6	1.03	23	.035
52.8	1.35	33	.051
53.0	1.04	50	.077

RUN 42 RH = .869 T = 25.0°C V = 24.0 cm sec⁻¹

42.0	.82	4	.0062
49.4	.97	10	.015
52.6	1.03	17	.026
53.0	1.04	32	.049

RUN 43 RH = .869 T = 25.0°C V = 24.0 cm sec⁻¹

43.2	.87	6	.0092
50.4	.99	13	.020
51.8	1.02	20	.031
52.8	1.35	30	.046
53.0	1.04	47	.072

RUN 43a RH = .886 T = 25.0°C V = 24.1 cm sec⁻¹

43.2	.87	4	.0062
49.9	.98	11	.017
52.6	1.03	17	.026
54.5	1.07	36	.055
55.2	1.08	52	.080

RUN 44 RH = .885 T = 25.0°C V = 24.1 cm sec⁻¹

46.8	.92	6	.0092
52.1	1.02	12	.019
52.8	1.04	17	.026
54.7	1.07	24	.037
55.2	1.08	33	.051

RUN 45 RH = .886 T = 25.0°C V = 24.1 cm sec⁻¹

<u>d = 2r</u>	<u>σ</u>	<u>t</u>	<u>τ</u>
46.8	.92	7	.011
52.3	1.03	15	.023
53.5	1.05	21	.032
54.96	1.08	30	.046
55.2	1.08	39	.060

RUN 46 RH = .904 T = 25.0°C V = 24.0 cm sec⁻¹

42.0	.82	3	.0046
51.6	1.01	10	.015
54.7	1.07	18	.028
55.9	1.10	27	.04
57.1	1.12	36	.055
57.6	1.13	47	.072

RUN 47 RH = .904 T = 25.0°C V = 24.0 cm sec⁻¹

45.4	.89	6	.0092
52.3	1.03	12	.018
54.7	1.07	20	.031
55.7	1.09	28	.043
57.1	1.12	37	.057
57.4	1.12	51	.079
57.6	1.13	62	.095

RUN 48 RH = .904 T = 25.0°C V = 24.0 cm sec⁻¹

45.6	.89	6	.0092
51.6	1.01	10	.015
54.0	1.06	16	.025
55.2	1.08	22	.034
56.2	1.10	28	.043
56.9	1.12	39	.060
57.6	1.13	60	.092

RUN 49 RH = .932-.934 T = 25.1-25.2°C V = 23.8 cm sec⁻¹

45.6	.89	6	.0092
52.8	1.04	11	.017
56.2	1.10	17	.026
59.3	1.16	25	.039
60.5	1.19	31	.048
62.2	1.22	42	.065
62.6	1.23	55	.085
64.1	1.26	67	.103
64.3	1.260	96	.148
64.6	1.27	129	.198

RUN 50 RH = .934 T = 25.2°C V = 23.8 cm sec⁻¹

<u>d = 2r</u>	<u>σ</u>	<u>t</u>	<u>τ</u>
40.8	.80	3	.0046
51.6	1.01	9	.014
55.7	1.09	15	.023
57.6	1.13	22	.034
61.2	1.20	32	.049
62.4	1.22	42	.065
63.6	1.25	53	.082
64.1	1.26	65	.10
64.8	1.27	100	.15

RUN 51 RH = .997-.999 T = 23.5-23.6°C V = est. 30-40 cm sec⁻¹

44.4	.87	5	.0077
62.4	1.22	16	.025
69.6	1.37	36	.055
75.8	1.49	65	.10
81.6	1.60	83	.13
85.2	1.67	114	.18
86.5	1.68	125	.19
91.2	1.79	155	.24
94.8	1.86	196	.30
98.5	1.93	231	.36
101	1.98	294	.45
105	2.06	335	.52
109	2.14	475	.73
113	2.22	521	.80
115	2.26	550	.85
117	2.30	614	.94
120	2.36	685	1.05

RUN 52 RH = .978-.982 T = 19.6-20.1°C V = est. 30-40 cm sec⁻¹

47	.92	5	.0070
58	1.14	13	.020
64	1.25	21	.032
66	1.29	31	.048
71	1.39	40	.062
76	1.49	60	.092
79	1.55	74	.11
82	1.61	94	.14
87	1.71	126	.19
89	1.74	145	.22
91	1.78	165	.25
94	1.84	199	.31
97	1.90	238	.38
99	1.94	267	.41
101	1.98	295	.45

RUN 52 RH = .978-.982 T = 19.6-20.1°C V = est. 30-40 cm sec⁻¹
(Contd.)

<u>d = 2r</u>	<u>σ</u>	<u>t</u>	<u>τ</u>
103	2.02	348	.54
106	2.08	412	.63
108	2.12	467	.72
110	2.16	521	.80
113	2.22	582	.90
115	2.25	667	1.03
118	2.32	745	1.15

RUN 53 RH = .978-.982 T = 20.6-20.9°C V = 26.5 cm sec⁻¹

48.0	.94	6	.0092
57.6	1.13	15	.023
64.4	1.26	24	.037
66.0	1.29	30	.046
74.2	1.45	55	.085
76.9	1.51	70	.11
81.5	1.60	95	.15
83.6	1.64	107	.16
86.5	1.70	138	.21
88.9	1.74	163	.25
91.2	1.79	183	.28
93.6	1.83	246	.38
96.0	1.88	307	.47

m = 910 $\mu\mu$ grams average

RUN 54 RH = .898 T = 25.0°C V = est. 30-40 cm sec⁻¹

19.9	1.02	5	.053
21.6	1.11	16	.170

RUN 55 RH = .898 T = 25.0°C V = est. 30-40 cm sec⁻¹

21.6	1.11	4	.043
------	------	---	------

RUN 56 RH = .898 T = 25.0°C V = est. 30-40 cm sec⁻¹

21.6	1.11	6	.064
------	------	---	------

RUN 57 RH = .938 T = 25.4-25.5°C V = est. 30-40 cm sec⁻¹

23.0	1.17	5	.053
24.5	1.26	14	.149
24.7	1.27	23	.244

RUN 58 RH = .959 T = 26.0-26.1°C V = est. 30-40 cm sec⁻¹

<u>d = 2r</u>	<u>σ</u>	<u>t</u>	<u>τ</u>
22.8	1.17	4	.043
27.6	1.41	12	.128
28.8	1.48	23	.244
29.3	1.50	35	.372
29.6	1.52	51	.54
30.0	1.54	84	.89

RUN 59 RH = .957-.959 T = 26.1°C V = est. 30-40 cm sec⁻¹

21.6	1.11	3	.032
27.6	1.41	12	.128
28.8	1.48	29	.308
29.3	1.50	37	.394
30.0	1.54	59	.63

RUN 60 RH = .980-.982 T = 26.6°C V = est. 30-40 cm sec⁻¹

22.8	1.17	3	.032
28.8	1.48	11	.117
31.2	1.60	21	.224
32.9	1.68	30	.320
33.6	1.72	40	.425
34.8	1.78	56	.595
35.8	1.84	72	.765
36.0	1.85	102	1.08

Technical Report Distribution List
ONR Project NR-085-001

20 March 1953

<u>Address</u>	<u>No. of Copies</u>
Chief of Naval Research, Navy Department, Washington 25, D. C. Attention: Code 416	3
Director, Naval Research Laboratory, Washington 25, D. C. Attention: Technical Information Officer, Code 2000	9
Director, Office of Naval Research Branch Office, 346 Broadway, New York 13, N. Y.	1
Director, Office of Naval Research Branch Office, 10th Floor, John Crerar Library Bldg., 36 E. Randolph St., Chicago 1, Illinois	1
Director, Office of Naval Research Branch Office, 1030 E. Green St., Pasadena 1, California	1
Director, Office of Naval Research Branch Office, 1000 Geary St., San Francisco, California	1
Director, Office of Naval Research Branch Office, 150 Causeway St., Boston, Massachusetts	2
Officer in Charge, Office of Naval Research, Navy #100, Fleet Post Office, New York, N. Y.	7
Department of Aerology, U. S. Naval Post Graduate School, Monterey, California	1
Aerology Branch, Bureau of Aeronautics (Ma-5), Navy Department, Washington 25, D. C.	1
Mechanics Division, Naval Research Laboratory, Anacostia Station, Washington 20, D. C. Attention: J. E. Dinger, Code 3820	1
Radio Division I, Code 3420, Naval Research Laboratory, Anacostia Station, Washington 20, D. C.	1
Meteorology Section, Navy Electronics Laboratory, San Diego 52, California, Attention: L. J. Anderson	1
Library, Naval Ordnance Laboratory, White Oak, Silver Spring 19, Maryland	1
Bureau of Ships, Navy Department, Washington 25, D. C., Attention: Code 851	1

Technical Report Distribution List
ONR Project NR-085-001

20 March 1953

<u>Address</u>	<u>No. of Copies</u>
Bureau of Ships, Navy Department, Washington 25, D.C., Attention: Code 814	1
Bureau of Ships, Navy Department, Washington 25, D. C., Attention: Code 327	2
Chief of Naval Operations, Navy Department, Washington, 25, D. C., Attention: OP-533D	2
Oceanographic Division, U. S. Navy Hydrographic Office. Suitland, Maryland	1
Library, Naval Ordnance Test Station, Inyokern, China Lake, California	1
Project AROWA, U. S. Naval Air Station, Bldg. R-48, Norfolk, Virginia	1
The Chief, Armed Forces Special Weapons Project, P. O. Box 2610, Washington, D. C.	1
Office of the Chief Signal Officer, Engineering and Technical Service, Washington 25, D. C., Attention: SIGGGM	1
Meteorological Branch, Evans Signal Laboratory, Belmar, New Jersey	1
Office of the Quartermaster General, 2nd and T Sts., Washington 25, D. C., Attention: Environmental Protection Section	1
Office of the Chief, Chemical Corps, Research and Engineering Division, Research Branch, Army Chemical Center, Maryland	2
Commanding Officer, Air Force Cambridge Research Cen- ter, 230 Albany St., Cambridge, Massachusetts. Attention: CRTSL-2	1
Headquarters, Air Weather Service, Andrews A. F. Base, Washington 20, D. C., Attention: Director Scientific Services	2
Commanding General, Air Material Command, Wright Field, Dayton, Ohio, Attention: MCREEO	1
Commanding General, Air Research and Development Com- mand, P. O. Box 1395, Baltimore 3, Maryland, Attention: RDDG	1

Technical Report Distribution List
ONR Project NR-085-001

20 March 1953

<u>Address</u>	<u>No. of Copies</u>
Department of Meteorology, Massachusetts Institute of Technology, Cambridge, Massachusetts, Attention: H. G. Houghton	1
Department of Meteorology, University of Chicago, Chicago 37, Illinois, Attention: H. R. Byers	2
Institute for Advanced Study, Princeton, New Jersey, Attention: J. von Neumann	1
Scripps Institution of Oceanography, La Jolla, California, Attention: R. Revelle	1
General Electric Research Laboratory, Schenectady, N.Y. Attention: I. Langmuir	1
St. Louis University, 3621 Olive St., St. Louis 8, Missouri, Attention: J. B. Macelwane, S. J.	1
Department of Meteorology, University of California at Los Angeles, Los Angeles, California, Attention: M. Neiburger	1
Department of Engineering, University of California at Los Angeles, Los Angeles, California, Attention: L.M.K. Boelter	1
Department of Meteorology, Florida State University, Tallahassee, Florida, Attention: W. A. Baum	1
Woods Hole Oceanographic Institution, Woods Hole, Massachusetts, Attention: C. Iselin	1
The Johns Hopkins University, Department of Civil Engineering, Baltimore, Maryland, Attention: R. Long	1
The Lamont Geological Observatory, Torrey Cliff, Palisades, N. Y., Attention: M. Ewing	1
The Johns Hopkins University, Department of Physics, Homewood Campus, Baltimore, Maryland, Attention: G. Plass	1
New Mexico Institute of Mining and Technology, Research and Development Division, Socorro, New Mexico. Attention: E. Workman	1
University of Chicago, Department of Meteorology, Chicago 37, Illinois, Attention: H. Riehl	

Technical Report Distribution List
ONR Project NR-085-001

20 March 1953

<u>Address</u>	<u>No. of Copies</u>
Woods Hole Oceanographic Institution, Woods Hole, Massachusetts, Attention: A. Woodcock	1
General Electric Research Laboratory, Schenectady, N. Y., Attention: V. Schaefer	1
Geophysical Institute, University of Alaska, College, Alaska, Attention: C. T. Elvey	1
Blue Hill Meteorological Observatory, Harvard Univer- sity, Milton 86, Massachusetts, Attention: C. Brooks	1
Department of Meteorology, University of Washington, Seattle 5, Washington, Attention: P. E. Church	1
Laboratory of Climatology, Johns Hopkins University, Seabrook, New Jersey, Attention: C. W. Thornwaite	1
Institute of Geophysics, University of California at Los Angeles, Los Angeles, California, Attention: J. Kaplan	1
Department of Meteorology, New York University, New York 53, N. Y., Attention: B. Haurwitz	1
Texas A and M, Department of Oceanography, College Station, Texas, Attention: J. Freeman, Jr.	1
Massachusetts Institute of Technology, Department of Meteorology, 77 Massachusetts Ave., Cambridge 39, Massachusetts, Attention: T. F. Malone	1
Cornell University, Department of Agronomy, Division of Meteorology, Ithaca, N. Y.	1
Pennsylvania State College, School of Mineral In- dustries, Department of Earth Science, State College, Pennsylvania, Attention: H. Neuberger	1
Rutgers University, College of Agriculture, Department of Meteorology, New Brunswick, New Jersey	1
University of Texas, Department of Aeronautical En- gineering, Austin, Texas, Attention: K. H. Jehn	1
University of Utah, Department of Meteorology, Salt Lake City, Utah, Attention: V. Hales	1

Technical Report Distribution List
ONR Project NR-085-001

20 March 1953

<u>Address</u>	<u>No. of Copies</u>
University of Wisconsin, Department of Meteorology, Madison, Wisconsin, Attention: V. Suomi	1
National Advisory Committee for Aeronautics, 1724 F St., N.W., Washington 25, D. C.	2
U. S. Weather Bureau, 24th and M Sts N.W., Wash- ington 25, D. C., Attention: Scientific Services Division	2
Committee on Geophysics and Geography, Research and Development Board, Washington 25, D. C.	2
Air Coordinating Committee, Subcommittee on Aviation Meteorology, Room 2D889-A, The Pentagon, Washing- ton, D. C.	1
American Meteorological Society, 3 Joy St., Boston 8, Massachusetts, Attention: The Executive Secretary	1
Research Professor of Aerological Engineering, College of Engineering, Department of Electrical Engineering, University of Florida, Gainesville, Florida	1
Professor Max A. Woodbury, Dept. of Statistics, Wharton School, University of Pennsylvania, Philadelphia 4, Pennsylvania	1
Stormy Weather Research Group, MacDonald Physics Lab- oratory, McGill University, Montreal 2, Quebec, Canada, Attention: Dr. Walter Hitschfeld	1
Dr. E. G. Bowen, Radio Physics Division, C.S.I.R.O., University Grounds, Sydney, New South Wales, Aus- tralia	1